การดูดซับโมเลกุลมีเทนและอีเทนบนพื้นผิว (010) ของซิลิกาไลต์-1 ที่ปกคลุมด้วยหมู่ซิลานอล:
ฟังก์ชันศักย์ฟิตจากแอบอินิชิโอ

นายรุ่งโรจน์ ฌานะจารี

วิทยานิพนธ์นี้เป็นส่วนหนึ่งของการศึกษาตามหลักสูตรปริญญาวิทยาศาสตรมหาบัณฑิต
สาขาวิชาเคมี ภาควิชาเคมี
คณะวิทยาศาสตร์ จุฬาลงกรณ์มหาวิทยาลัย
ปีการศึกษา 2549

ADSORPTIONS OF METHANE AND ETHANE MOLECULES ON SILANOL
COVERED SILICALITE-1 (010) SURFACE: AB INITIO FITTED POTENTIAL

Mr. Rungroj Chanajaree

A Thesis Submitted in Partial Fulfillment of the Requirements

for the Degree of Master of Science Program in Chemistry

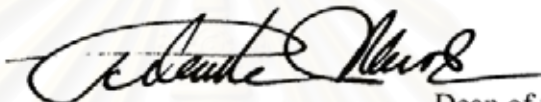Department of Chemistry

Faculty of Science

Chulalongkorn University

Academic year 2006

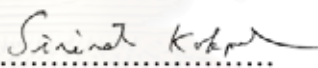Thesis Title   ADSORPTIONS OF METHANE AND ETHANE
                    MOLECULES ON SILANOL COVERED
                    SILICALITE-1 (010) SURFACE: AB INITIO FITTED
                    POTENTIAL
By   Mr. Rungroj Chanajaree
Field of Study   Chemistry
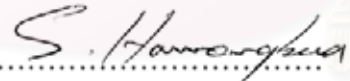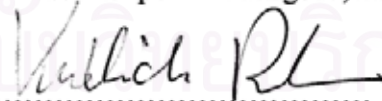Thesis Advisor   Professor Supot Hannongbua, Ph. D.

_____

    Accepted by the Faculty of Science, Chulalongkorn University in Partial
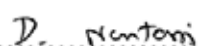Fulfillment of the Requirements for the Master's Degree

    .... Dean of the Faculty of Science
    (Professor Piamsak Menasveta, Ph. D.)

THESIS COMMITTEE

    .... Chairman
    (Associate Professor Sirirat Kokpol, Ph. D.)

    .... Thesis Advisor
    (Professor Supot Hannongbua, Ph. D.)

    .... Member
    (Associate Professor Vudhichai Parasuk, Ph. D.)

    .... Member
    (Duangamol Nuntasri, Ph. D.)

    .... Member
    (Associate Professor Tawan Sooknoi, Ph. D.)

รุ่งโรจน์ ฌานะจารี: การดูดซับโมเลกุลมีเทนและอีเทนบนพื้นผิว (010) ของซิลิกาไลต์-1 ที่ปกคลุมด้วยหมู่ซิลานอล: ฟังก์ชันศักย์ฟิตจากแอบอินิชิโอ (ADSORPTIONS OF METHANE AND ETHANE MOLECULES ON SILANOL COVERED SILICALITE-1 (010) SURFACE: AB INITIO FITTED POTENTIAL) อ. ที่ปรึกษา: ศ. ดร. สุพจน์ หารหนองบัว, 68 หน้า.

ได้ศึกษารูปแบบพลังงานอันตรกิริยาระหว่างเกสต์โมเลกุลซึ่งได้แก่มีเทนและอีเทนกับพื้นผิว ของซิลิกาไลต์-1 (010) ที่ปกคลุมด้วยหมู่ซิลานอล ด้วยวิธีทางกลศาสตร์ควอนตัมแอบอินิชิโอ ONIOM(MP2/6-31G(d):HF/6-31G(d)) ที่รวมการแก้ไขความคลาดเคลื่อนเนื่องจากการซ้อนทับของ เบซิสเซต (BSSE) ทั้งนี้ พื้นผิวซิลิกาไลต์-1 (010) เตรียมจากพื้นผิวส่วนที่ตั้งฉากกับท่อตรงของ โครงสร้างผลึกอุดมคติของซีโอไลต์ MFI หมู่ซิลานอลบนพื้นผิวนั้นสร้างโดยเติมอะตอมไฮโดรเจนที่ พันธะ –Si-O- ที่อยู่บนพื้นผิว จากนั้นได้นำพลังงานที่ได้จากการคำนวณวิธีออเนียมมาสร้างเป็นฟังก์ชัน ศักย์ ผลการทดสอบพบว่าพลังงานที่ได้จากการคำนวณวิธีออเนียมและจากฟังก์ชันศักย์ สอดคล้องกัน เป็นอย่างดี ผลการวิเคราะห์ยังพบว่าวิธีการเคลื่อนที่ที่ดีที่สุดสำหรับเกสต์โมเลกุลที่จะผ่านเข้าสู่ท่อตรง คือบริเวณกึ่งกลางของท่อตรง โดยโครงสร้างของมีเทนที่ดีที่สุดคือชี้ไฮโดรเจนหนึ่งอะตอมไปยังพื้นผิว และตั้งฉากกับพื้นผิว โดยมีพลังงานยึดเหนี่ยว -5.75 กิโลจูลต่อโมล ส่วนพลังงาน ยึดเหนี่ยวสำหรับอี เทนในโครงสร้างที่ชี้พันธะ C-C ไปยังพื้นผิวและตั้งฉากกับพื้นผิวคือ -10.92 กิโลจูลต่อโมล นอกจากนี้ ยังได้ทดสอบคุณภาพของฟังก์ชันศักย์ที่พัฒนาขึ้น โดยนำไปใช้ในการจำลองพลวัตเชิงโมเลกุล ใน วิทยานิพนธ์ระดับปริญญาเอกของ "ถมโพธิ์" ซึ่งพบว่าได้ผลเป็นที่น่าพอใจ

ภาควิชา............เคมี............ลายมือชื่อนิสิต..

สาขาวิชา............เคมี............ลายมือชื่ออาจารย์ที่ปรึกษา..............................

ปีการศึกษา..........2549..........

4772439523: MAJOR CHEMISTRY
KEY WORD: SILICALITE / SILANOL / POTENTIAL FUNCTION / ONIOM /
MOLECULAR DYNAMICS SIMULATIONS

RUNGROJ CHANAJAREE: ADSORPTIONS OF METHANE AND ETHANE MOLECULES ON SILANOL COVERED SILICALITE-1 (010) SURFACE: AB INITIO FITTED POTENTIAL. THESIS ADVISOR: PROF. SUPOT HANNONGBUA, Ph.D., 68 pp.

The interaction profiles between guest molecules, methane and ethane, and the silanol covered (010) silicalite-1 surface have been investigated using quantum *ab initio*, ONIOM (MP2/6-31G(d):HF/6-31G(d)) method including the correction due to the basis set super position error (BSSE). The silicalite-1 (010) surface, which perpendicular to the straight channel was selected and cut from an idealized MFI crystal lattice. The silanol groups on the surface were generated by adding hydrogen atoms to the broken –Si-O- bonds. The ONIOM energy data were fitted to an analytical function. Quality of the fitted function was, then, examined. The energetic data obtained from the two sources, ONIOM and fitted function, are in good agreement for both methane/silicalite-1 and ethane/silicalite-1 systems. It was also found that the optimal path for guest molecule to enter the straight channel is that at the center of the channel. The optimal orientation for methane is to point one H atom at the center and perpendicular to the surface leading to the binding energy of -5.75 kJ/mol. The corresponding energy for ethane is -10.92 kJ/mol in the configuration where the C-C bond points toward and perpendicular to the surface. The fitted potential function was examined by Thompho's Ph.D. thesis using molecular dynamics (MD) simulations in order to validate the fitted functions. Reliability of the functions was clearly yielded.

Department	Chemistry	Student's signature	
Field of study	Chemistry	Advisor's signature	
Academic year	2006		

ACKNOWLEDGEMENTS

CONTENTS

Pages

Pages

LIST OF FIGURES

LIST OF TABLES

CHAPTER I

INTRODUCTION

1.1. Research Rationale

1.1.1 Zeolites

A "molecular sieve" is a material with selective adsorption properties capable to separate components of a mixture on the basis of a difference in molecular size and shape[1]. The sieves include clays, porous glasses, microporous charcoals, active carbons, zeolites, etc.

Zeolites are microporous aluminosilicate materials which have numerous properties that are appropriate for catalysis and separation. The high porosity and very regular system of pores lead to be beneficial characteristics of these materials as for example shape selectivity and catalytic properties.

Hydrocarbons in zeolites are of particular interested to the petrochemical industrials, and this has been an active area of research. ZSM-5 and its free aluminum silicalite-1, have been widely studied. The main channels of ZSM-5/silicalite-1 are 10-membered oxygen rings with diameter of about 5.5 Å. They could help to improve performance in many industrial processes such as a separation of the hydrocarbons from mixtures, hydrocarbon catalytic cracking isomerization, alkylation of hydrocarbon, and alcohol conversion to gasoline.

1.1.2 The Silanol on the External Surface

The zeolite external surface area is key factor that affects its catalytic performance. Almost applications of zeolites typically begin with the initial adsorption of molecules on the external surface followed by diffusion on the external surface and sieving of the molecules into the internal surface. Therefore, the external surface area of ZSM-5/silicalite-1 is a parameter of great industrial importance and should be measured and optimized for various applications. The key elements

determining the adsorption and diffusion behavior of guest molecules on the external surfaces are silanol groups. The FTIR technique is mostly used to characterize the silanol on the external surface. However, most of the experiment and theoretical works focus on the internal surface, whereas much less detail of the external surface.

1.1.3 The *Ab Initio* Fitted Potentials

It is well known that quality and reliability of the simulation results rely on the use of the intermolecular potential employed, in which the previous studies are based on molecular mechanics (MM) parameterization[2-4]. This potential energy surface is usually generalized to be applicable for a wide range of molecular systems, leading to lack of some specific details. *Ab initio* derived interaction potential would be more appropriate, especially for the present case, where hydrogen bonding can be quantum mechanically parameterized to higher precision. Recently, such intermolecular potential were developed and successively applied to study structure, dynamics and thermodynamics properties of the guest-silicalite-1 systems[5, 6].

1.2. Zeolites

1.2.1. What a Zeolite is

In 1756 Cronstedt[7], a Swedish mineralogist, described zeolites for the first time. He proposed the term "zeolite" (in translation from Greek "a boiling stone"). Other minerals of this family such as mordinite, faujasite, chabasite possess similar properties. Zeolites[8-10] can be found in nature and these natural zeolites are seldom phase-pure and contain impurities of other minerals. Synthetic zeolites are manufactured from chemicals, and they hold some key advantages over their natural analogies. It is also possible to manufacture synthetic zeolite structures, which do not appear in nature.

Zeolites are porous crystalline aluminosilicalites. The three-dimentional zeolite network consists of SiO_4 and AlO_4^- tetrahedral linked together by sharing oxygen atoms[11]. Zeolite may be described with the followings empirical formula[12]:

$$M_{2/n}^{n+} \cdot AlO_2^- \cdot xSiO_2 \cdot yH_2O \tag{1.1}$$

Where M - counterion

                 n - counterion valence

                 x - silicon/aluminium ratio

                 y - content of hydrate water
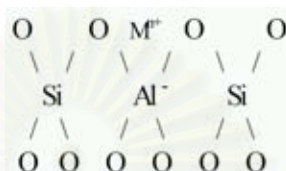
Figure 1.1 Basic structure of zeolites

In addition to Si^{4+} and Al^{3+}, other elements can also be presented in the zeolitic framework. They need not be isoelectronic with Si^{4+} or Al^{3+}, but must be able to occupy framework sites. Aluminosilicate zeolites display a net negative framework charge, but other molecular sieve frameworks may be electrically neutral.

1.2.2. Classification of Zeolites

Zeolites are divided into different structure type groups, which are different in channel geometry[13]. The channels can be elliptical, circular, and tubular or contain periodic cavities, straight or zig-zag. The pore structure in zeolites is determined by the framework, composition and cation presence[14]. Zeolites pore sizes are in the range of 3-10 Å. Originally, zeolites are named by Framework Type Codes which are identification by three capital letters used by the International Zeolite Association (IZA). The primary building unit of a molecular sieve is the individual tetrahedral unit. The topology of all known molecular sieve framework types can be described in terms of a finite number of specific combinations of tetrahedra called "secondary building units" (SBU's)[15]. In the Figure 1.2 the T atom belonging to a TO_4 tetrahedron is located at each corner, but the oxygens located near the mid-points of the lines joining each pair of T atoms are not shown[16]. A molecular sieve framework is made up of one type of SBU only.
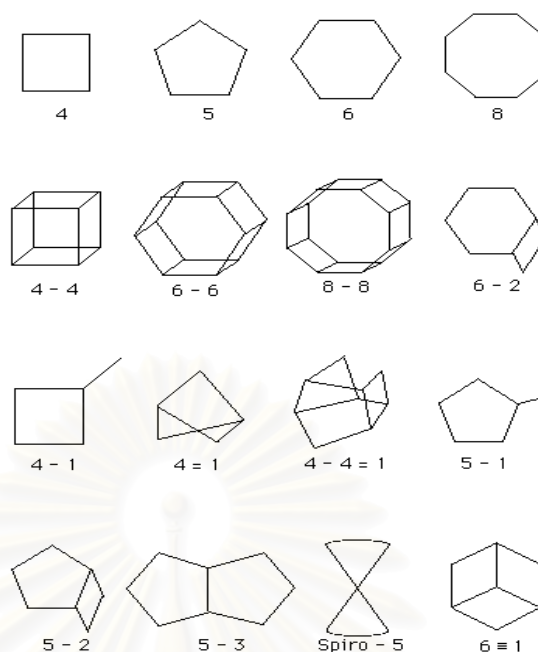
Figure 1.2 Secondary building units (SBU's) found in zeolite-like molecular sieve structures.

These secondary building units consist of 4, 6, and 8-member single rings, 4-4, 6-6, and 8-8-member double rings, and 4-1, 5-1, and 4-4-1 branched rings. The tetrahedron units can be arranged in rings, chains, sheets or complex frameworks taking into account various types and sizes of cavities that lead to their different properties for each zeolite. Generally, zeolites can also be classified, according to their pore sizes, into small, medium, large and ultralarge pore systems. The corresponding number of tetrahedral (membered ring) are 6, 8, 9 for small; 10 for medium; 12 for large; and 14, 18, 20 for ultralarge structures. The characteristics of some typical zeolites are listed in Table 1.1.

Table 1.1 Characteristics of some typical porous materials[17].

Zeolite	Number of rings	Pore size (Å^2)	Pore/channel structure
8-membered oxygen ring			
Erionite	8	3.6x5.1	Intersecting
10-membered oxygen ring			
ZSM-5	10	5.1x5.6	Intersecting
		5.1x5.6	
ZSM-11	10	5.3x5.4	Intersecting
Dual pore system			
Ferrierite	10,8	4.2x5.4	One dimensional
		3.5x4.8	10:8 intersecting
Mordenite	12	6.5x7.0	One dimensional
	8	2.6x5.7	12:8 intersecting
12-membered oxygen ring			
ZSM-12	12	5.5x5.9	One dimensional
Faujasite	12	7.4	Intersecting
		7.4x6.5	12:12 intersecting
Mesoporous system			
VPI-5	18	12.1	One dimensional
MCM41-S	-	16-100	One dimensional

1.2.3. Applications

Zeolites have found widespread industrial applications as highly selective adsorbents, ion exchangers and, most importantly, catalysts of exceptionally high activity and selectivity in a wide range of reactions[10]. These applications include the drying of refrigerants, removal of atmospheric pollutants such as sulphur dioxide, separation of air components, separation and recovery of normal paraffin hydrocarbons, recovering radioactive ions from waste solutions, catalysis of hydrocarbon reactions and the curing of plastics and rubber. Zeolites exhibit appreciable Brønsted acidity with shape-selective features not available in amorphous catalysts of similar composition.

Molecular sieves are selective, high-capacity adsorbents because of their high intracrystalline surface area and strong interactions with adsorbates. Molecules of different size generally have different diffusion properties in the same molecular sieve. Molecules are separated on the basis of size and structure relative to the size and geometry of the apertures of the sieve. Molecular sieves adsorb molecules, in particular those with a permanent dipole moments, and exhibit other interactions not

found in other sorbents. Different polar molecules have a different interaction with the molecular sieve framework, and may thus be separated by a particular molecular sieve. This is one of the major uses of zeolites. An example is the separation of N_2 and O_2 in the air on zeolite A, by exploiting different polarities of the two molecules[10]. The quantity of adsorbed gas or liquid depends on pressure, temperature, the nature of the adsorbate and the kind of the molecular sieve. Variations in the chemical composition of the sieve also affect adsorption. The adsorbed molecules can be removed by heating and/or evacuation. It is also known that the aluminium in materials such as VPI-5 may possess a higher coordination member than four, indicating that chemisorptions of water occurs[18-20]. The structure may also be changed while the adsorbed water is driven away.

The ring sizes of molecular sieve may be determined by sorption of molecules of different size[10]. Water and nitrogen are two of the smallest molecules which can easily penetrate almost the entire structures. These two molecules are normally used to determine the crystallinity of molecular sieves by comparing the adsorption volume with that of a standard sample.

Zeolites with low Si/Al ratios have strongly polar anionic frameworks. The exchangeable cations create strong local electrostatic fields and interact with highly polar molecules such as water. The cation-exchange behaviour of zeolites depends on (*i*) the nature of the cation species, the cation size (both anhydrous and hydrated) and cation charge, (*ii*) the temperature, (*iii*) the concentration of the cationic species in the solution, (*iv*) the anion associated with the cation in solution, (*v*) the solvent (most exchange has been carried out in aqueous solutions, although some work has been done in organics), and (*vi*) the structural characteristics of the particular zeolite.

Cation exchange in a zeolite is accompanied by an alteration of stability, adsorption behaviour and selectivity, catalytic activity and other properties. In some cases, the introduction of a larger or smaller cation will decrease or enlarge the pore opening. The location of that cation within the crystal will also contribute to the size of pore opening. For example, the Na^+ form of zeolite A has a smaller effective pore dimension than would be expected for its 8-membered ring framework opening. This is due to sodium ion occupancy of sites where it will partially block the 8-membered ring window. When the Na^+ ion is exchanged for the larger K^+ ion, the pore diameter is reduced so that only the very small polar molecules will be adsorbed. If the divalent Ca^{2+} cation is used to balance of the framework charge, the effective pore opening

widens, as only half the number of cations are needed. These ions occupy sites within the voids of the zeolite and do not reduce the effective pore diameter of the 8-membered ring. Highly and purely siliceous molecular sieves have virtually neutral frameworks, exhibit a high degree of hydrophobicity and no ion-exchange capacity.

The most important application of molecular sieves is as catalysts. Zeolites combine high acidity with shape selectivity, high surface area and high thermal stability. They have been used to catalyze a variety of hydrocarbon reactions, such as cracking, hydrocracking, alkylation and isomerisation. The reactivity and selectivity of zeolites as catalysts are determined by the active sites brought about by a charge imbalance between the silicon and aluminium atoms in the framework. Each framework aluminium atom induces a potential active acid site. In addition, purely siliceous and $AlPO_4$ molecular sieves have Brønsted acid sites whose weak acidity seems to be caused by the presence of terminal -OH bonds on the external surface of the crystal.

Shape selectivity, including reactant shape selectivity, product shape selectivity or transition-state shape selectivity, plays a very important role in molecular sieve catalysis. The channels and cages in a molecular sieve are similar in size to medium-sized molecules. Different sizes of channels and cages may therefore promote the diffusion of different reactants, products or transition-state species. High crystallinity and the regular channel structure are the principal features of molecular sieve catalysts. Reactant shape selectivity results from the limited diffusivity of some of the reactants, which cannot effectively enter and diffuse inside the crystal. Product shape selectivity occurs when slowly diffusing product molecules cannot rapidly escape from the crystal, and undergo secondary reactions. Restricted transition-state shape selectivity is a kinetic effect arising from the local environment around the active site: the rate constant for a certain reaction mechanism is reduced if the necessary transition state is too bulky to form readily.

1.2.4. Silicalite-1

MFI, A and FAU types are the most common structures in research and industry. The channels in the MFI structure are formed by five-member ring building units liked together (Figure 1.3)[21]. These building units render a framework of

sinusoidal channels in the a-direction and straight channels in the b-direction with slightly elliptical pore openings.
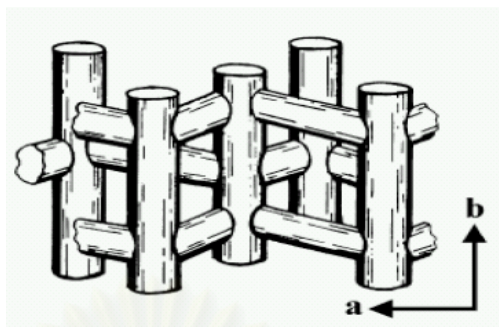
Figure 1.3 The MFI channel system with crystallographic axis.

Two well-know MFI structure are silicalite-1 and ZSM-5. The difference between them is the aluminium content. ZSM-5 has Si/Al ratio in the range[22] 10-200, when this ratio is more than 200, the material is denoted silicalite-1. Silicalite-1 is a structural analogue to the ZSM-5 zeolite, but due to the fact that silicalite-1 does not contain aluminium or only very small amount. This material therefore exhibits non-polar characteristics such as low reactivity and hydrophobicity. It should be noted that the internal surface of perfect silicalite-1 is hydrophobic, whereas the external surface is hydrophilic. For this reason, silicalite-1 is an attractive adsorbent for the separation of relatively non-polar species from aqueous media, e.g., the separation of mixtures of light hydrocarbons with water or other polar solvents, the removal of organic compounds from automobile exhaust and the recovery of alcohols from aqueous solutions. This can be attributed to terminal silanol groups which are able to interact with guest molecules. It is known that the key elements determining the adsorption and diffusion behavior of guest molecules on the external surface are silanol groups.

1.3. Silanols

Several mineral classifications are based on the SiO_4 unit and its manifold ways of condensation. Extensive work has been carried out on silicates and their structural and geometrical principles and properties, to understand, quantify and predict the silicate structures. The SiO_4 and H in minerals rarely bond to each other to form SiOH group (silanol group). H atoms usually bond to an O atom of a higher-

coordinated cation, and the hydrogen bond is one of the most important chemical linkages in nature.

Silanol is a hydroxyl group that is connected with a silicon atom (Si-OH). Silanol are usually classified into three types[23], namely, *(i)* the isolated silanol groups, *(ii)* the vicinal pair, where silanol groups can form hydrogen bonds with each other and *(iii)* the germinal species, where two hydroxyls sit on the same Si atom.
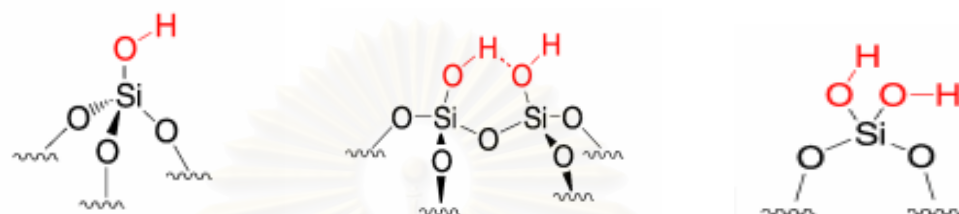
Isolated silanol group   **Vicinal silanol groups**   **Geminal silanol groups**

Figure 1.4 Three types of silanol groups.

The average bond length of the non-hydroxylated Si-O bonds (Si-O) is 1.618 Å. In contrast to the more expanded average Si-O bond length of the silanol group (Si-OH) is 1.643 Å. The Si-OH distance decreases with the number of bridging O atoms from average values of 1.668 Å for orthosilicates to 1.604 Å for tetrahedral with three bridging O atoms, whereas the Si-O distance remains constant at 1.62 Å.

Silanol groups existing on the outer surfaces of zeolites, whose OH stretching band appears at the same frequency as that of silanol groups on amorphous silica, are recognized as neutral or very weakly acidic. It was found that isobutene molecules could not adsorb on the acidic OH groups of ferrierite and ZSM-5, and that a reaction occurred when they adsorbed on silanol groups. This evidences the higher reactivity of silanol groups on ferrierite and ZSM-5 than of those on amorphous. Therefore, they could be concluded to be slightly more acidic than those on amorphous silica. The difference in acid strength of silanol groups is most probably attributed to the slight stress due to the inclusion of silanol groups in the highly crystallized structures of zeolites, although they exist on the external surface[23].

There are two kinds of terminal silanol groups in zeolites: *(i)* the bridging Si-(OH)-Al hydroxy groups and *(ii)* Si-OH at the external surface. The experiments confirmed that two kinds of terminal silanol groups, indistinguishable from the point of view of the OH stretching band but differing in their Brønsted acidity, are located

at the external surface of the ZSM-5 zeolite crystals, no evidence was found for the presence of bridging Si-(OH)-Al sites at the external surface of the ZSM-5 zeolite samples. The shape selectivity (pore size), density and type of Brønsted acid sites are considered to affect the diffusion process. The geometry of the pores leads to the formation of hydrogen bonding interactions between these silanol groups. Several FTIR experiments prove that the O-H bond of silanol groups is softened when interacting with nitriles, alcohols, water, pyridine and with aliphatic and aromatic hydrocarbons[24, 25]. However, most of the experimental and theoretical works focus on the internal surface, which means the pore or channel, whereas much less is known about the details of the external surface.

1.4. The Zeolite External Surface

The surfaces of MFI zeolites can be separated into two parts: (*i*) the internal surface comprising the walls of the channels and the intersections and (*ii*) the external surface comprising the pore openings and the framework surface between the pore opening on the outside of the crystals (Figure 1.5). The external surface accounts for typical MFI zeolite crystals with sizes of ca. 1 µm. For example, the external surface areas (ESA) account for only 4.5% and 0.26% of the total surface area, for ZSM-5 zeolite crystals with sizes of ca. 2 µm and 10 µm, respectively[26].
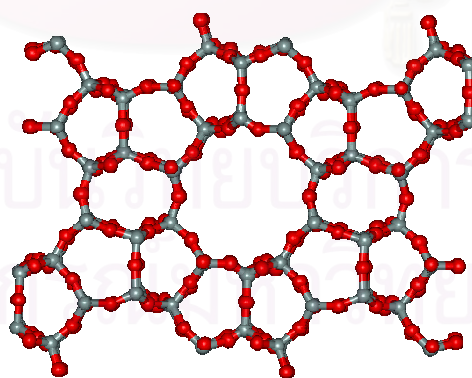
Figure 1.5 The (010) external surface of silicalite-1.

The zeolite external surface area (ESA) is an important parameter that affects its catalytic performance. Applications of zeolites typically begin with the initial adsorption of molecules (from the gas phase or the liquid phase) on the external surface of a zeolite crystal followed by diffusion on the external surface and sieving of the molecules into the internal surface. The size/shape selective catalysis can be classified into two major categories: (*i*) diffusion-controlled size/shape selectivity depending on the relative rates of diffusion of reagents into the internal surface or product out of the internal surface and (*ii*) transition-state selectivity in the confined environment of the zeolite channels and their intersections[27]. In either case, the size/shape selective reactions are mainly associated with the reactions that take place in the zeolite internal surface. Reactions on the external surface typically do not proceed in a size/shape selective manner. Therefore, assuming a comparable catalytic reactivity of the reagents on the internal and external surface, zeolite crystals with larger crystal sizes and consequently smaller ESA per unit mass will possess higher catalytic size/shape selectivity. However, the ESA is directly proportional to the concentration of the pore openings, which in turn affects the velocity of diffusion of reagent molecules into the channels or the product molecules out of the channels. As a result, the size/shape selective catalysis in the internal surface proceeds at a lower rate for larger crystals because of limitations on diffusion of the guest molecules, and side reactions could become more pronounced when the desired reaction is diffusionally retarded. Therefore, the ESA of an MFI zeolite is a parameter of great industrial importance and should be measured and optimized for various applications[28].

1.5. Hydrocarbons in Zeolites

Reactions of hydrocarbons in zeolites are of the greatest interest since these are the reactions catalyzed by zeolites in oil refinement, and this has been an active area of research. Zeolites could help to improve performance in many industrial processes such as separation of the hydrocarbons from mixtures, hydrocarbon catalytic cracking, isomerization, alkylation of hydrocarbon, and alcohol conversion to gasoline[29-31]. The knowledge of where a particular alkane will adsorb is of great benefit to the industrial use of zeolites since it is the adsorption of certain alkanes that will degrade the catalytic performance of a zeolite. Recently, there have been several

computational studies on different guests (including hydrocarbons) adsorbed in zeolites[32, 33].

Molecular dynamics (MD) simulation has been proved to be a useful tool and widely used to investigate the molecular diffusion in zeolites. It mostly contributes to the understanding of microscopic mechanism of the diffusion processes. Nevertheless, MD simulation is quite time-consuming, limiting its applicability to small systems and time scales and thus to the systems with molecular dynamics studies up to now have been focused on the diffusion of small linear alkanes in zeolites.

Methane diffusion in zeolites has been the subject of a number of computer modeling studies. Demontis et al.[34, 35] and Goodbody et al.[36] studied methane diffusion in silicalite by using the model where the guest molecules were regarded as soft spheres. Demontis et al.[4] simulated methane diffusion in ZSM-5 and the results are in good agreement with the experimental results. It was found that the lattice flexibility is not affect the diffusion of small guest molecules. June et al.[37] studied methane silicalite at four different loadings and three different temperatures, and found that at 300 and 400 K, methane self-diffusion monotonically decrease with the increasing of the loading, while at 200 K, self-diffusivities first reach a weak maximum and then decrease at high loading. Nicholus et al.[2] investigated methane diffusion in silicalite at infinite dilution and the loading of 2, 4, 8, 12 and 16 molecules per unit cell. The calculated self-diffusion constant range is in excellent agreement with the PFG NMR result. It was found that guest-silicalite and guest-guest interactions have effects on the packing of methane molecules in silicalite. The isosteric heat of adsorption of methane was -5.8 kcal/mol, in good agreement with the experimental result from adsorption isotherm method. Flexible methane molecules in ZSM-5 and silicalite were simulated by Catlow et al.[38] and Dumont et al.[39], respectively. The computed diffusion coefficients are both in acceptable agreement with the experimental data. The motion of methane in faujasite, silicalite and sodium-A can also be found in the literatures [37, 40-42].

Nowak et al.[43] simulated the diffusion of rigid ethane molecules in rigid silicalite, reporting the computed diffusion coefficient as 4.7×10^{-9} m^2/s, which is in good agreement with the PFG NMR result. Flexible ethane in rigid silicalite framework was investigated by Dumont et al.[39]. The theoretical diffusion coefficient was 5.9×10^{-9} m^2/s which is a little bigger than the experimental value. Demontis et al.[44] simulated flexible ethane molecules in flexible silicalite. Both the

computed heat of adsorption and diffusion coefficient agree with the experimental data. It was found that a molecule with lower vibrational frequency diffused slightly lower. Caro *et al.*[45] simulated the diffusion of ethane in ZSM-5 and zeolite NaX, observing a monotonous decreasing in the self-diffusion coefficients with the increasing of molecular concentration. Dumont *et al.*[39] studied the vibrational spectrum of flexible ethane in silicalite, obtaining very satisfactory structure and diffusion data.

1.6. Scope of This Study

This study aims to develop intermolecular potential function to represent interaction between the silanol covered silicalite-1 (010) surface and guest molecules (methane and ethane) using *ab initio* data. In addition, interaction energies were intensively investigated in order to seek for their optimal binding site on the silicalite-1 surface. Here, some hundreds of methane and ethane positions on the silicalite-1 surface were calculated at the ONIOM(MP2/6-31G(d):HF/6-31G(d)) levels in which an error due to unbalance of the basis set used, the basis set super position error (BSSE), were also included. The obtained potentials were examined by Thompho (Ph.D. thesis) using molecular dynamics simulations in order to investigate transportation processes of methane and ethane molecules into the pore of silicalite-1 through the silanol covered (010) external surface.

CHAPTER II

THEORY

2.1 Quantum Mechanics

2.1.1 Introduction

Wavefunction is the basic of quantum mechanics (QM) which is the correct mathematical description of the behavior of electrons and thus of chemistry. In theory, QM can predict any property of an individual atom or molecular exactly. In practice, the QM equations could only be solved exactly for one electron systems. A multitude collection of methods has been developed for approximating the solution for multiple electron systems. These approximations can be very useful, but this requires an amount of sophistication on the part of the researcher to know when each approximation is valid and how accurate the results are likely to be.

2.1.2 *Ab Initio* Methods

The term *ab initio* is Latin for "from the beginning". This name is given to computations that are derived directly from theoretical principles without experimental data. This is an approximate quantum mechanical calculation. The approximations made are usually mathematical approximations, such as using a simpler functional form for a function or finding an approximate solution to a differential equation.

2.1.2.1 Schrödinger Equation

$$\hat{H}\psi(q_i, q_\alpha) = E\psi(q_i, q_\alpha) \tag{2.1}$$

where $\hat{H}$ is Hamiltonian operator, ψ the wave function, E the energy, q_i and q_α symbolize the electronic and nuclear coordinates, respectively. The probability distribution of the particles within the molecule is interpreted by $|\psi|^2$.

The Hamiltonian $\hat{H}$, like the energy in classical mechanics, is the sum of kinetic and potential operators.

$$\hat{H} = -\frac{\hbar^2}{2}\sum_\alpha \frac{1}{m_\alpha}\nabla_\alpha^2 - \frac{\hbar^2}{2m_e}\sum_i \nabla_i^2 + \sum_\alpha \sum_{\beta>\alpha} \frac{Z_\alpha Z_\beta e^2}{r_{\alpha\beta}} - \sum_\alpha \sum_i \frac{Z_\alpha e^2}{r_{i\alpha}} + \sum_j \sum_{i>j} \frac{e^2}{r_{ij}} \quad (2.2)$$

where α and β refer to nuclei, m_e and m_α refer to electron mass and nuclear mass, and i and j refer to electrons. The first term in (2.2) is the operator for kinetic energy of the nuclei. The second term is the operator for the kinetic energy of the electrons. The third term is the potential energy of the repulsions between the nuclei, $r_{\alpha\beta}$ being the distance between nuclei α and β with atomic numbers Z_α and Z_β. The fourth term is the potential energy of the attractions between the electrons and the nuclei, $r_{i\alpha}$ being the distance between electron i and nucleus α. The last term is the potential energy of the repulsions between the electrons r_{ij} being the distance between electron i and j. The zero level of potential energy for (2.2) corresponds to having all the charges (electrons and nuclei) infinitely far from one another.

2.1.2.2 The Born-Oppenheimer Approximation

The key lies in the fact that nuclei are much heavier than electrons: $m_\alpha \gg m_e$. Hence the electrons move much faster than nuclei, and to a good approximation as far as the electrons are concerned, we can regard the nuclei as fixed while the electrons carry out their motions. Speaking classically, during the time of a cycle of electronic motion, the change in nuclear configuration is negligible. Thus, considering the nuclei as fixed, we omit the nuclear kinetic-energy terms from (2.2) to obtain the Schrödinger equation for electronic motion:

The *purely electronic Hamiltonian $\hat{H}_{el}$* is

$$\hat{H}_{el} = -\frac{\hbar^2}{2m_e}\sum_i \nabla_i^2 - \sum_\alpha \sum_i \frac{Z_\alpha e^2}{r_{i\alpha}} + \sum_j \sum_{i>j} \frac{e^2}{r_{ij}} \qquad (2.3)$$

The electronic Hamiltonian including nuclear repulsion is $\hat{H}_{el} + V_{NN}$. The nuclear-repulsion term V_{NN} is given by

$$V_{NN} = \sum_\alpha \sum_{\beta > \alpha} \frac{Z_\alpha Z_\beta e^2}{r_{\alpha\beta}} \qquad (2.4)$$

The approximation of separating electronic and nuclear motions is called the *Born-Oppenheimer approximation* and is the basic to quantum chemistry.

2.1.2.3 Spatial Orbitals and Spin Orbitals

We define an orbital as a wave function for a single particle, an electron. Because we are concerned with molecular electronic structure we will be using molecular orbitals for the wave functions of the electrons in a molecule. A spatial orbital $\psi_i(\mathrm{r})$, is a function of the position vector r and describes the spatial distribution of an electron such that $|\psi_i(\mathrm{r})|^2 d\mathrm{r}$ is the probability of finding the electron in the small volume element $d\mathrm{r}$ surrounding r. Spatial molecular orbitals will usually be assumed to form an orthonormal set

$$\int d\mathrm{r}\, \psi_i^*(\mathrm{r})\psi_j(\mathrm{r}) = \delta_{ij} \qquad (2.5)$$

If the set of spatial orbitals $\{\psi_i\}$ were complete, then any arbitrary function $f(\mathrm{r})$ could be exactly expanded as

$$f(\mathrm{r}) = \sum_{i=1}^{\infty} a_i \psi_i(\mathrm{r}) \qquad (2.6)$$

The wave function for an electron that describes both its spatial distribution and its spin is a spin orbital, $\chi(\mathrm{x})$, where x indicates both space and spin coordinates.

$$\chi(\mathrm{x}) = \begin{cases} \psi(\mathrm{r})\alpha(\omega) \\ \text{or} \\ \psi(\mathrm{r})\beta(\omega) \end{cases} \tag{2.7}$$

2.1.2.4 The Hartree-Fock Approximation

The Hartree-Fock approximation constitutes the first step towards more accurate approximations. The simplest antisymmetric wave function, which can be used to describe to ground state of an *N*-electron system, is a single Slater determinant,

$$\Psi_0 = |\chi_1 \chi_2 \cdots \chi_N\rangle \tag{2.8}$$

where $\chi_i(\mathrm{r}_i, \omega_i)$ is the spin orbital which depends on spatial coordinate r and spin function ω. The variation principle states that the best wave function of this functional form (Equation 2.9) is the one which gives the lowest possible energy. The energy of this wave function, expressed in term of the set of spin orbitals $\{\chi_i | i = 1, 2, \ldots, N\}$, is given by (Equation 2.10),

$$E_0 = \langle \Psi_0 | \hat{H} | \Psi_0 \rangle \tag{2.9}$$

$$E_0 = \sum_i^N (i|h|i) + \frac{1}{2} \sum_i^N \sum_j^N (ii|jj) - (ij|ji) \tag{2.10}$$

For a closed-shell system, the wave function (Equation 2.8) contains $N/2$ spin orbitals with α spin function and $N/2$ spin orbitals with β spin fuction (Equation 2.10) can be written as

$$E_0 = 2 \sum_i^{N/2} (i|h|i) + \sum_{ij}^{N/2} 2(ii|jj) - (ij|ji) \tag{2.11}$$

First, consider the one-electron terms

$$(i|h|i) = h_{ii} = \int d\mathbf{r}\, \psi_i^*(\mathbf{r}_1)(-\frac{1}{2}\nabla_1^2 - \sum_{k=1}^{M}\frac{Z_k}{r_{1k}})\psi_i(\mathbf{r}_1) \tag{2.12}$$

Thus h_{ii} is the average kinetic and nuclear attraction energy of an electron described by the wave function $\psi_i(\mathbf{r}_1)$. Next consider the two-electron integral

$$(ii|jj) = \int d\mathbf{r}_1 d\mathbf{r}_2 |\psi_i(\mathbf{r}_1)|^2 \frac{1}{r_{12}} |\psi_j(\mathbf{r}_2)|^2 \tag{2.13}$$

which is the classical coulomb repulsion between the charge clouds $|\psi_i(\mathbf{r}_1)|^2$ and $|\psi_j(\mathbf{r}_2)|^2$. Thus, this integral is called a *coulomb* integral and is denoted by

$$J_{ij} = (ii|jj) = \langle ij|ij \rangle \tag{2.14}$$

Finally, consider the two-electron integral

$$(ij|ji) = \int d\mathbf{r}_1 d\mathbf{r}_2 \psi_i^*(\mathbf{r}_1)\psi_j(\mathbf{r}_1)\frac{1}{r_{12}}\psi_j^*(\mathbf{r}_2)\psi_i(\mathbf{r}_2) \tag{2.15}$$

This integral does not have classical interpretation. It is called an *exchange* integral and is denoted by

$$K_{ij} = (ij|ji) = \langle ij|ji \rangle \tag{2.16}$$

Both exchange and coulomb integrals have positive values. Rewrite the Hartree-Fock energy of a closed-shell system in terms of coulomb and exchange integrals, we obtained

$$E_0 = 2\sum_a h_{ii} + \sum_{ij} 2J_{ij} - K_{ij} \tag{2.17}$$

The variational flexibility in the wave function (Equation 2.8) is in the choice of spin orbitals. By minimizing E_0 with respect to the choice of spin orbitals, one can derive an equation, called the Hartree-Fock equation, which determines the optimal spin orbitals. The Hartree-Fock equation is an equation of the form

$$f(i)\chi(\mathrm{x}_i) = \varepsilon\chi(\mathrm{x}_i) \qquad (2.18)$$

where $f(i)$ is an effective one-electron operator, called the Fock operator. The Fock operator has the form

$$f(i) = -\frac{1}{2}\nabla_i^2 - \sum_{k=1}^{M}\frac{Z_k}{r_{ik}} + v^{\mathrm{HF}}(i) \qquad (2.19)$$

where $v^{\mathrm{HF}}(i)$ is the average potential experienced by the ith electron due to the presence of the other electrons. The essence of the Hartree-Fock approximation is to replace the complicated many electron problem by a one-electron problem in which electron-electron repulsion is treated in an average way. The procedure for solving the Hartree-Fock equation is called the self-consistent field (SCF) method.

The basic idea of the SCF method is simple. By making an initial guess at the spin orbitals, one can calculate the average field (*i.e.*, v^{HF}) seen by each electron and then solve the eigenvalue equation (Equation 2.18) for a new set of spin orbitals. Using these new spin orbitals, one can obtain new fields and repeat the procedure until self-consistency is reached (*i.e.*, until the fields no longer change and the spin orbitals used to construct the Fock operator are the same as its eigenfunctions), as in Figure 2.1.
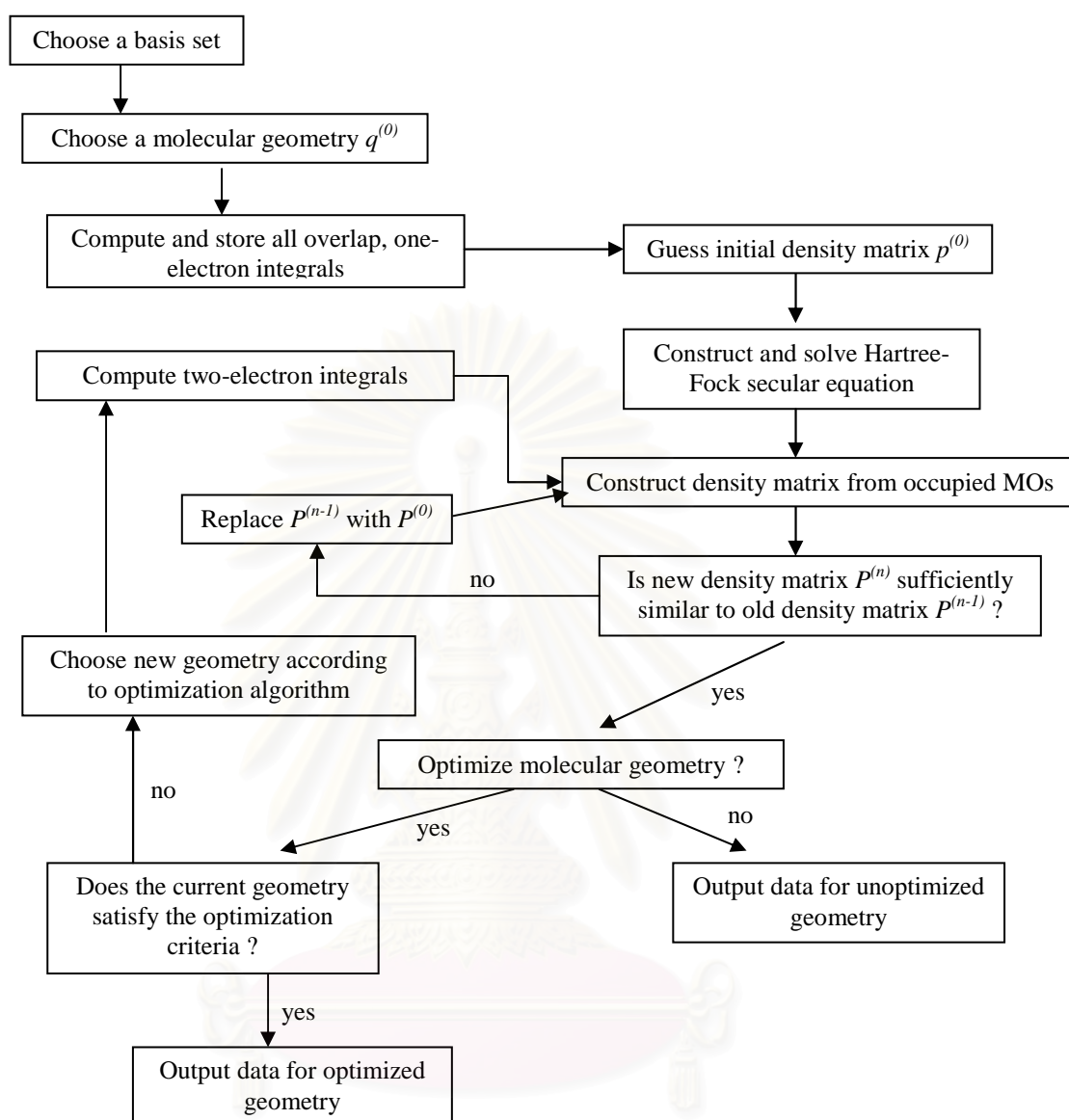
Figure 2.1 Flow chart of the HF SCF procedure. Note that data for an unoptimized geometry is referred to as deriving from a so-called 'single point calculation'

The solution of the Hartree-Fock eigenvalue problem (Equation 2.18) yields a set $\{\chi_k\}$ of orthonormal Hartree-Fock spin orbitals with orbital energies $\{\varepsilon_k\}$. The N spin orbitals with the lowest energies are called the occupied or hole spin orbitals. The Slater determinant formed from these orbitals is the Hartree-Fock ground state wave function and is the best variational approximation to the ground state of the system, of the single determinant form.

The Hartree-Fock equation can also be solved by introducing a finite set of spatial basis functions $\{\phi_\mu(r)|\mu = 1,2,\ldots,K\}$. The spatial parts of the spin orbitals with the α and β spin function can then be expanded in terms of the known set of functions $\{\phi_\mu\}$ by using a basis set of K spatial functions $\{\phi_\mu\}$ leads to a set of $2K$ spin orbitals (K with α spin K and with β spin).

$$\psi_i = \sum_{i=1}^{2K} C_{\mu_i} \phi_\mu \tag{2.20}$$

2.1.2.5 Møller-Plesset Perturbation Theory

Møller-Plesset perturbation theory is a tool of perturbation theory, which provides a method for adding excitations to the Hartree-Fock wavefunction and therefore including the effect of electron correlation. The first-order energy is exactly the HF energy. To obtain an improvement on the HF energy it is therefore necessary to use *Møller-Plesset* perturbation theory at least second order. This level of theory is referred to as MP2. The higher-order wave function is expressed as linear combinations of solutions to the zeroth-order Hamiltonian:

$$\Psi_0^{(1)} = \sum_j c_j^{(1)} \Psi_j^0 \tag{2.21}$$

The $\Psi_j^{(0)}$ in (2.21) will include single, double, etc. excitations obtained by promoting electron into the virtual orbitals obtained from a HF calculation. The second-order energy is given by:

$$E_0^{(2)} = \sum_i \sum_{j>1}^{occupied} \sum_a \sum_{b>a}^{virtual} \frac{\int\int d\tau_1 d\tau_2 \chi_j(2)(\frac{1}{r_{12}})[\chi_a(1)\chi_b(2) - \chi_b(1)\chi_a(2)]}{\varepsilon_a + \varepsilon_b - \varepsilon_i - \varepsilon_j} \qquad (2.22)$$

This is important for the Van der Waals bond between rare gas atoms and non-polar molecules, also significantly to other types of intermolecular bonding, e.g. hydrogen bonds.

These integral will be non-zero only for double excitations, according to the Brillouin theorem. Third- and fourth-order Møller-Plesset calculations (MP3 and MP4) are also available as standard options in many *ab initio* packages.

2.1.2.6 Basis Sets

Slater and Gaussian Type Orbitals

There are two types of basis functions. The first one is so-called Slater-Type Orbitals (STOs). It is defined as

$$\Phi_{STO}(\varsigma, n, l, m; r, \theta, \phi) = Nr^{n-1}e^{-\varsigma r}Y_{lm}(\theta, \phi) \qquad (2.23)$$

where N is a normalization constant, ς is called "exponent". The r, θ and ϕ are spherical coordinates, and Y_{lm} is the angular momentum part which is a function describing the "shape". The n, l and m are principal, angular momentum and magnetic quantum numbers, respectively. Due to using STO's, two-electron integrals are difficult and time consuming to evaluate. To speed up molecular integral evaluation, Boys proposed in 1950 the use of Gaussian-Type Orbitals (GTOs) instead of STOs for the atomic orbital in an LCAO wave function. These orbitals decay as functions of $e^{-\alpha r^2}$. The functional form for GTO's is expressed as:

$$g(\alpha, l, m, n; x, y, z) = Ne^{-\alpha r^2}x^a y^b z^c \qquad (2.24)$$

where N is a normalization constant, α is called "exponent". x, y, z are Cartesian coordinates. a, b and c are simply integral exponents at Cartesian coordinates ($r^2 = x^2$

+ y^2 + z^2). Each group of basis functions can be treated as a unit called a *contracted Gaussian-Type Orbitals, CGTOs*. Constituent Gaussians making up a contracted Gaussian are called primitive Gaussians or simply primitives. In using many Gaussian to express the space part of a molecular orbital, one finds that demands on computer resources increase roughly as the fourth power of the number of basis function. Hence, one should keep the number of basis function as small as possible.
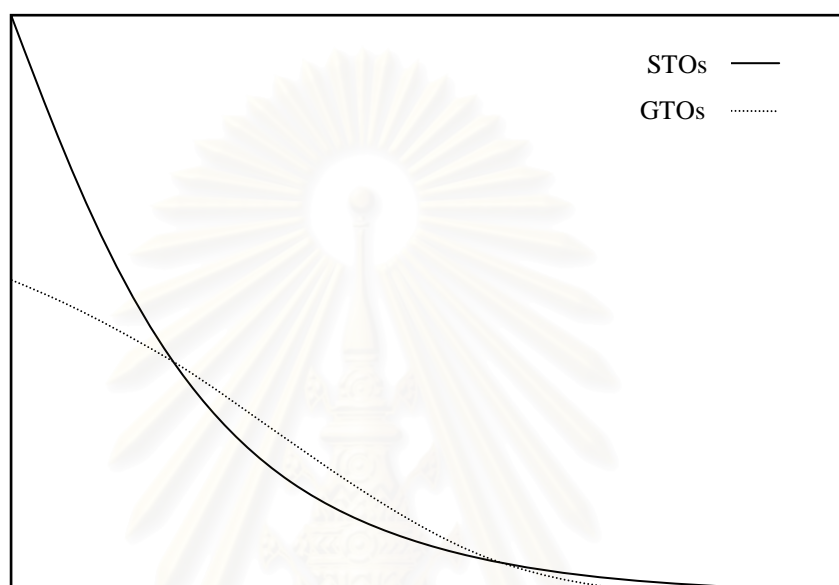
Figure 2.2 Comparison of Slater and Gaussian functions

The r^2 dependence in the exponential makes the GTOs inferior to the STOs in two aspects. At the nucleus the GTOs has zero slope, in contrast to the STOs which has a "cusp" (discontinuous derivative), and GTOs have problems representing the proper behavior near the nucleus. The other is that the GTOs falls off too rapidly far from the nucleus compared with an STOs, and the "tail" of wave function is consequently represented poorly. A rough guideline says that three times as many GTOs as STOs are required for reaching a given level of accuracy. In terms of computational efficiency, GTOs are therefore preferred, and used almost universally as basis functions in electronic structure calculations.

Classification of Basis Sets

Single-ζ, Multiple-ζ, and Split-Valence

The STO-3G basis set is known as a "single-ζ" basis set, or, more commonly, a "*minimal*" basis set. There is one basis function defined for each type of orbital core through valence (e.g. 1s for H and He; 1s, 2s, 2px, 2py, 2pz for Li to Ne). Because the minimal basis set is so small, it is not recommended for consistent and accurate predictions of molecular energies. However, their simple structure provides a good tool for visualizing qualitative aspects of chemical bonding.

One way to increase the flexibility of a basis set is to "decontract" it. We could construct two basis functions for each AO, the first being a contraction of the first two primitive Gauassians, while the second would simply be the normalized third primitive. A basis set with two functions for each AO is called a "double-ζ" basis. Of course, we could decontract further, and treat each primitive as a full-fledged basis function, in which case we would have a "triple-ζ" basis, and we could then decide to add more functions indefinitely creating higher and higher multiple-ζ basis sets.

The reason that core orbitals are only weakly affected by chemical bonding, on the other hand, valence orbitals can vary widely as a function of chemical bonding. Atoms bonded to significantly more electronegative elements take on partial positive charge from loss of valence electrons, and thus their remaining density is distributed more compactly. The more cost effective way to improve the basis set is to have more flexibility for the valence electrons only, the recognition of this phenomenon led to the development of so-called "split-valence" or "valence-multiple-ζ" basis sets. The core orbitals are represented by minimal basis set whereas the valence shell orbitals are represented by more than one basis function such as 3-21G, 6-21G, 4-31G, and 6-31G, which have one contracted Gaussian function that is a linear combination of three primitive Gaussian functions for each inner-shell atomic orbital and two basis functions, one contracted Gaussian function that is a linear combination of two primitive Gaussians and one primitive Gaussian function, for each valence orbital. If there is valence-triple-ζ, like 6-311G, use three sizes of contracted functions for each orbital-type.

Polarization Functions

Polarized basis sets allow some small contributions from the unfilled orbital, what is required for the ground state for atom description by adding orbitals with angular momentum beyond. Pople and co-workers introduced a simple nomenclature scheme to indicate the presence of these functions, the "*" (star). Thus, 6-31G* implies a set of d functions added to polarized the p functions in 6-31G. A second star implies p functions on H and He, e.g., 6-31G**. To use more than one set of polarization functions in modern calculation, the standard nomenclature for the Pople basis sets now typically includes an explicit enumeration of those functions instead of the star nomenclature. Thus, 6-31G(d) is to be preferred over 6-31G* because the former obviously generalizes to allow names like 6-31(3d2fg,2pd), which implies heavy atoms polarized by three sets of d function, two sets of f functions, and of g functions, and hydrogen atoms by two sets of p functions and one of d. There is no limit on the number of polarization functions included in the basis set, however, it does increase the computational demand significantly.

Diffuse Functions

When a basis set does not have the flexibility necessary to allow a weakly bound electron to localize far from the remaining density (such as molecules with lone pairs, anions and other systems with significant negative charge, systems in their excited states, and system with low ionization potentials), significant errors in energies and other molecular properties can occur. In the Pople family of basis sets, the presence of diffuse functions is indicated by a "+" in the basis set name. The 6-31G+G(d) indicates that heavy atoms have been augmented with an additional one s and one set of p functions having small exponents. A second plus indicates the presence of diffuse s functions on H, e.g., 6-311++G(3df,2pd).

2.1.2.7 Basis Set Superposition Error

Suppose we wish to calculate the energy of formation of a bimolecular complex, such as the energy of formation of a hydrogen-boned water dimer. Such complexes are sometimes referred to as "supermolecules". One might expect that this energy value could be obtained by first calculating the energy of a single water molecule, then calculating the energy of the dimer, and finally subtracting the energy of the two isolated water molecules (the "reactants") from that of the dimer (the "product"). However, the energy difference obtained by such an approach will invariably be an overestimate of the true value. The discrepancy arises from a phenomenon known as *basis set superposition error* (BSSE). As the two water molecules approach each other, the energy of the system falls not only because of the favorable intermolecular interactions but also because the basis function on each molecule provide a better description of the electronic structure around the other molecule. It is clear that the BSSE would be expected to be particularly significant when small, inadequate basis sets are used which do not provide for an adequate representation of the electron distribution far from the nuclei, particularly in the region where non-covalent interactions are strongest. One way to estimate the basis set superposition error is via the counterpoise correction method of Boys and Bernardi, in which the entire basis set is included in all calculations [Boys and Bernardi 1970]. Thus, in the general case:

$$A + B \rightarrow AB \qquad (2.25)$$

$$\Delta E = E(AB) - [E(A) + E(B)] \qquad (2.26)$$

The calculation of the energy of the individual species A is performed in the presence of "ghost" orbitals of B; that is, without the nuclei or electrons of B. A similar calculation is performed for B using ghost orbitals on A. An alternative approach is to use a basis set in which the orbital exponents and contraction coefficients have been optimized for molecular calculations rather than for atoms. The relevance of the basis set superposition error and its dependence upon the basis set and the level of the theory employed (i.e. SCF or with electron correlation) remains a subject of much research.

2.1.2.8 The ONIOM (Our own *N*-layered Integrated molecular Orbital and molecular Mechanics) Approach

The ONIOM method[46-51] is an onion skin-like extrapolation method. At the beginning, Morokuma *et al.* proposed the Integrated Molecular Orbital and Molecular Mechanics (IMOMM) method which partitioned the system into 2 parts where different levels of theory are treated. Afterwards, it was realized that the extrapolation scheme in a combined MO + MO method, which was referred to as the Integrated Molecular Orbital and Molecular Orbital Method (IMOMO). Subsequently, the integration of more than two methods was succeeded, and the whole series of integrated methods was named the ONIOM method. Hence, IMOMO encompasses both two-layered ONIOM2 (MO:MO) and three-layered ONIOM3 (MO:MO:MO), and IMOMM is in principle equivalent to ONIOM2 (MO:MM) and ONIOM3 (MO:MO:MM). Thus, interesting or difficult part of the system is treated with more accurate method while the remains of the system are treated with the less accurate method. By this approach, a lot of computation time can be saved and "real" instead of "model" system can be studied. The crucial aspect in this and other hybrid schemes is the interaction between this inner and the outer part (higher level of theory)/(lower level of theory) of the system.

Hybrid Calculations with ONIOM

In the two-layered ONIOM method, the total energy of the system is obtained from three independent calculations:

$$E^{ONIOM2} = E_{real}^{low} - E_{model}^{low} + E_{model}^{high}$$

(2.27)

where *real* denotes the full system, which is treated at the *low* level, while *model* denotes the part of the system for which the energy is calculated at both *high* and *low* levels. The concept of the ONIOM method is represented schematically in Figure 2.3. One can see that method can be regarded as an extrapolation scheme. Beginning at E_{model}^{low}, the extrapolation to the high-level calculation ($E_{model}^{high} - E_{model}^{low}$) and the

extrapolation to the real system ($E_{real}^{low} - E_{model}^{low}$) are assumed to produce an estimate for E_{real}^{high}.

(A)
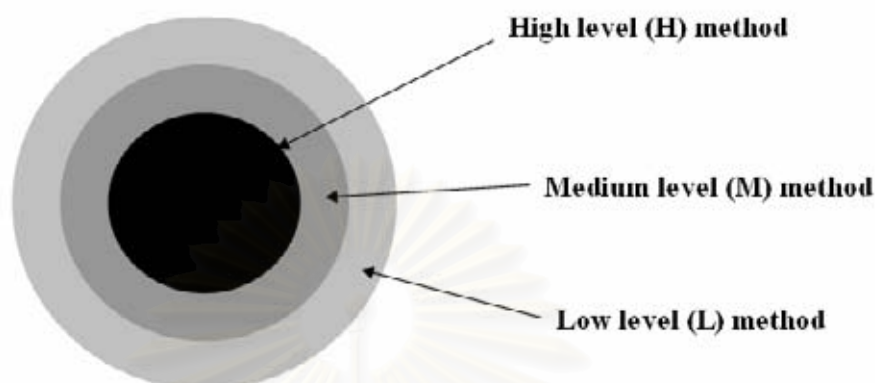
(B)
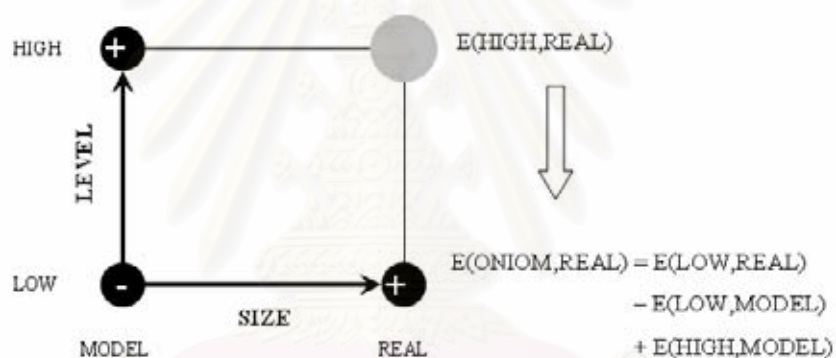
(C)

Figure 2.3 Schematic representation of: (A) The onion skin-like layers and models. (B) The two-layered ONIOM extrapolation scheme. (C) Three-layered ONIOM extrapolation scheme.

As can be seen, there is no restriction on the methods used at various levels (high, medium, low), and various MO and MM combination discussed above can be derived. Combining different levels of MO methods is a unique feature of the ONIOM method. It turns out that MO:MO integration is rather straightforward, and virtually no special attention is required. On the other hand, the integration in ONIOM of MO and MM methods, co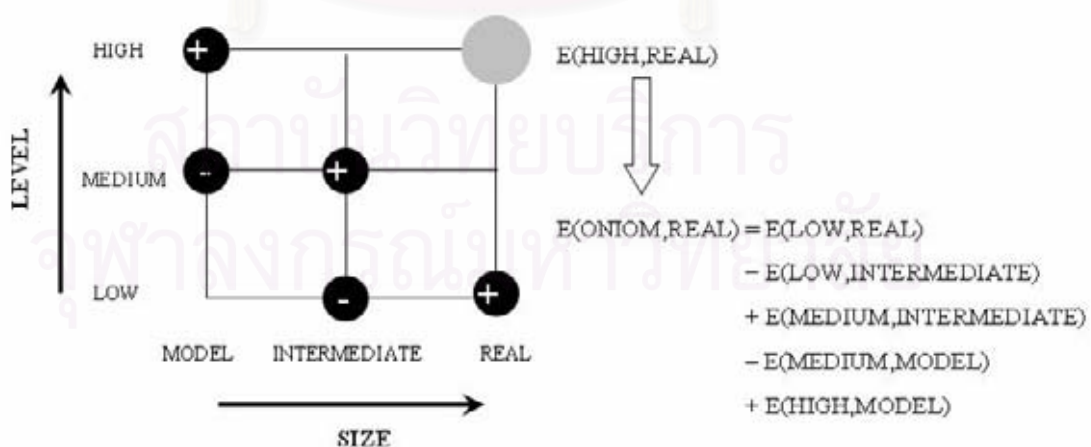mbining two methods with very different philosophies, lead to many serious problems, as with all of the QM/MM methods. The integration of two MO levels with one MM level, ONIOM3 (MO:MO:MM), is unique, a feature absent from other QM/MM methods. In MO-MM combinations, the interaction between the MO and MM regions can be treated at the MM level, i.e., with so-called mechanical embedding, or, alternatively, in the QM Hamiltonian, with so-called electron embedding.

2.2 The Lennard-Jones and Coulomb Pair Potential

The dispersive and exchange-repulsive interactions between atoms and molecules can be calculated using a simple empirical expression that can be rapidly calculated van der Waals interaction. The very famous potential function in molecular dynamics (MD) is the *Lennard-Jones (L-J) 12-6 function*[52]. It was proposed in 1931 by John Lennard-Jones of Bristol University. The L-J potential is of the form

$$v(r) = 4\varepsilon \left[\left(\frac{\sigma}{r} \right)^{12} - \left(\frac{\sigma}{r} \right)^{6} \right] \tag{2.28}$$

The Lennard-Jones potential contains interatomic separation (r) and just two adjustable parameters which are the collision diameter σ (the separation for which the energy is zero) and the energy constant ε (or well depth). These parameters are shown in Figure 2.4. The Lennard-Jones equation may also be expressed in terms of the separation at which the energy passes through a minimum, $r_m = 2^{1/6}\sigma$. It can also be written as follows:

$$v(r) = \varepsilon \left\{ \left(\frac{r_m}{r} \right)^{12} - 2 \left(\frac{r_m}{r} \right)^{6} \right\} \tag{2.29}$$

or

$$v(r) = \frac{A}{r^{12}} - \frac{B}{r^6}$$ (2.30)

where coefficient A is equal to εr_m^{12} (or $4\varepsilon\sigma^{12}$) and coefficient B is equal to $2\varepsilon r_m^6$ (or $4\varepsilon\sigma^6$)
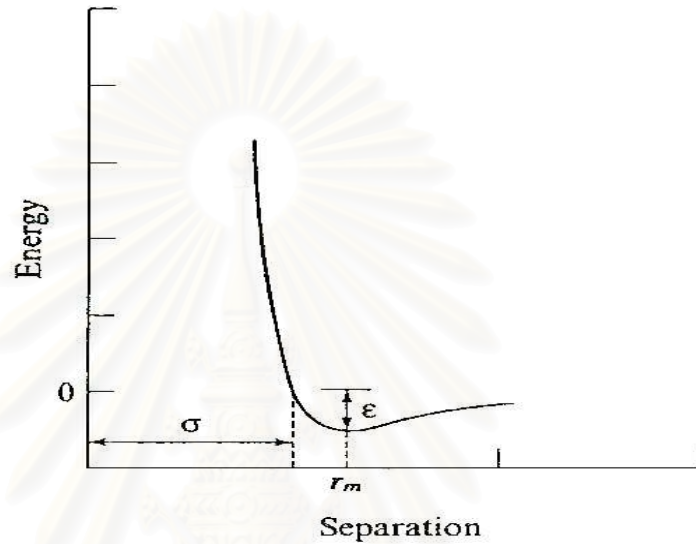
Figure 2.4 The Lennard-Jones potential

The term $\left(\frac{1}{r}\right)^{12}$, describes repulsion and the $\left(\frac{1}{r}\right)^6$ term describes attraction. The form of the repulsion term has no strong theoretical justification. The L-J formula is more convenient due to the ease and efficiency of computing r^{12} as the square of r^6. The attractive long-range potential is derived from dispersion interactions. These two components are shown in Figure 2.5.
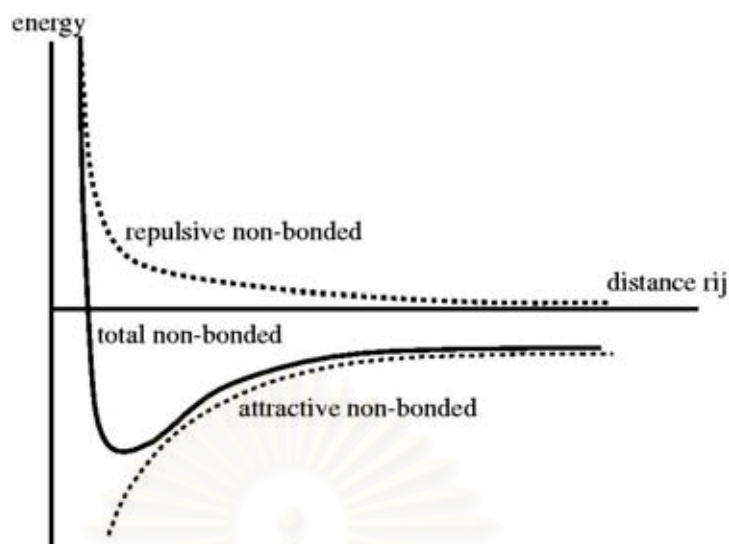
Figure 2.5 The Lennard-Jones potential is constructed from a repulsive and an attractive component

Another part of the interaction is the Coulomb potential, which is an effective pair potential that describes the interaction between two point charges. These charges are designed to reproduce the electrostatic properties of the molecule. If the charges are restricted to the nuclear centers they are often referred to as *atomic net charges*. The electrostatic interaction between two molecules (or different part of the same molecule) is then calculated as a sum of interactions between pairs of point charges using Coulomb's law:

$$v(r) = \frac{q_i q_j}{r} \tag{2.31}$$

where r is the distance between two atoms, q_i and q_j are the atomic net charges of atom i and j in atomic unit.

CHAPTER III

CALCULATION DETAILS

3.1 Quantum Chemical Calculations and Potential Functions Development

In this chapter, interaction energies between guest molecules and the external surface of the silanol covered (010) silicalite-1 were carried out using *ab initio* calculations. Then, the energy data points were fitted to the analytical function. The detailed method and the basis set used were illustrated as follow.

3.1.1 The Surface Model of Silicalite-1

The (010) external surface of the silicalite-1 perpendicular to the straight channel, was selected. The idealized MFI crystal lattice shown in Figure 3.1a was chosen as starting structure. It was, respectively, cut as indicated by the dashed line in Figure 3.1a and the circle in Figure 3.1b. The silanol groups on the surface were generated by adding hydrogen atoms as "terminators" to the broken -Si-O- bonds. With this procedure, the chemical composition after filling up the remaining valence orbitals of the silicon atoms with electron from hydrogen atoms, is $O_{86}Si_{32}H_{44}$. The positions of the hydrogen atoms were fully optimized using quantum chemical calculations at the HF/6-31G(d) level, i.e., change of the OH bond length as well as their rotations were allowed to be changed with respect to the total energy of the system. The obtained fragment, as shown in Figure 3.1c, was used throughout.
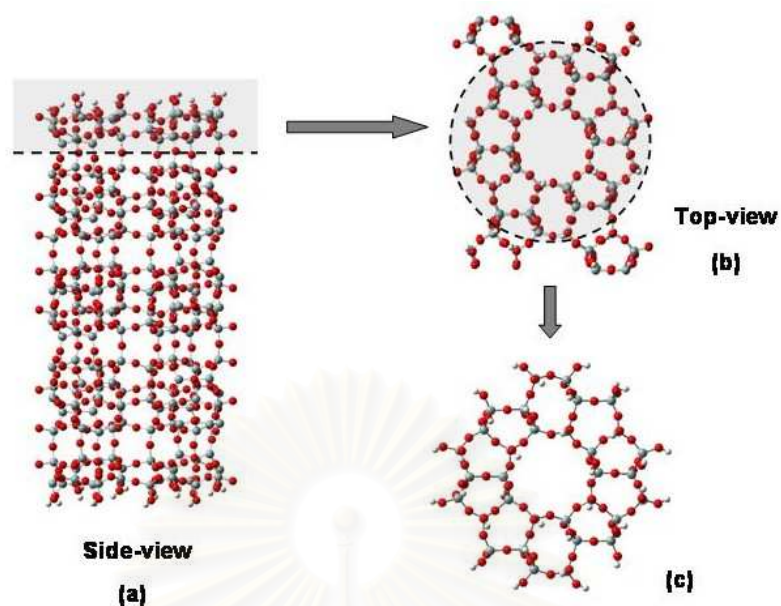
Figure 3.1 Side-view (a) and top-view (b) of the (010) surface which was cut as indicated by the dashed line and the circle. After adding silanol (-OH) group to the surface and energy minimization (detail see text) the obtained fragment (c) was used to represent the silanol covered (010) silicalite-1 surface.

3.1.2 Development of Guest Molecules/Silicalite-1 Potential Functions

In order to develop intermolecular potential functions representing the interaction between two molecules in all configurations, numerous coordinates of the second molecule around the first one had been generated. Subsequently, the interaction energies of configurations will be calculated using ONIOM method. The obtained data points must then be fitted to an analytical form.

The high accuracy level, MP2, which is shown to be a capable method for the nonpolar covalent molecules[53-55], was applied in this study. Due to the size of obtained fragment which is still too large to take into account all atoms in the MP2 calculations. The ONIOM (MP2/6-31G(d):HF/6-31G(d)) calculation with the BSSE correction[55] was used throughout in order to investigate the interaction between the guest molecules and the silanol covered (010) silicalite-1 surface.

Figure 3.2 shows the model part (ball-and-stick style) and the real part (all atoms) for the ONIOM calculations. The low level, HF/6-31G(d) method and the more accurate MP2/6-31G(d) method were applied to calculate the model part

whereas the real part was treated by low level method, HF/6-31G(d). The ONIOM interaction energy of the system, ΔE_{ONIOM} can be estimated extrapolatively from three independent calculations as:

$$\Delta E_{ONIOM} = E(_{real,\ low}) + E(_{model,\ high}) - E(_{model,\ low}) \tag{3.1}$$

where $E_{(real,\ low)}$ is the total energy of the real system using the low level method, while $E_{(model,\ high)}$ and $E_{(model,\ low)}$ denote the total energies of the model part calculated with high and low level methods, respectively.
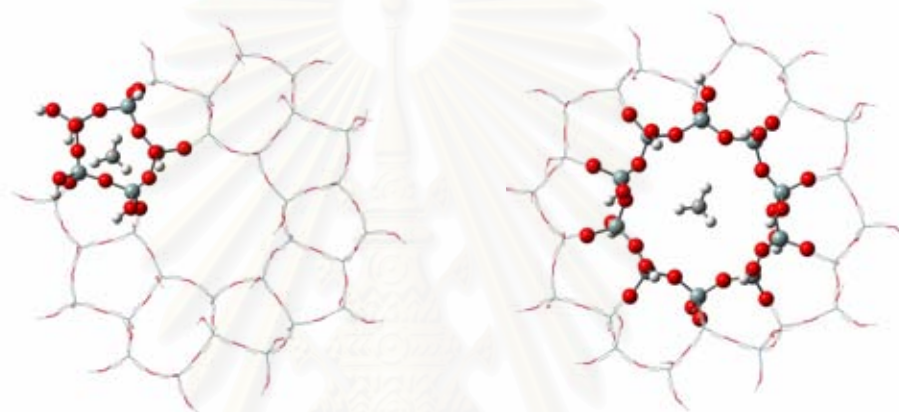
Figure 3.2 The real part and the model part which used for the ONIOM method.

In order to reduce the scope of the calculation, the methane molecule in the two orientations (H-in and H-out) and the ethane molecule in the two orientations (perpendicular and parallel) were positioned at several points, above the (010) silicalite-1 surface and in the trajectory perpendicular to the surface. The distance from the center of mass of guest molecules to point i, where $i = 1$-7 labeled in Figure 3.3, were varied.

1. Center of the 5-membered ring
2. Center of the 6-membered ring
3. O of Si-O-Si
4. O on 10-membered ring
5. O of H-O-Si
6. H of H-O
7. Center of the 10-membered

a)

H-out   **H-in**

b)

Perpendicular   **Parallel**
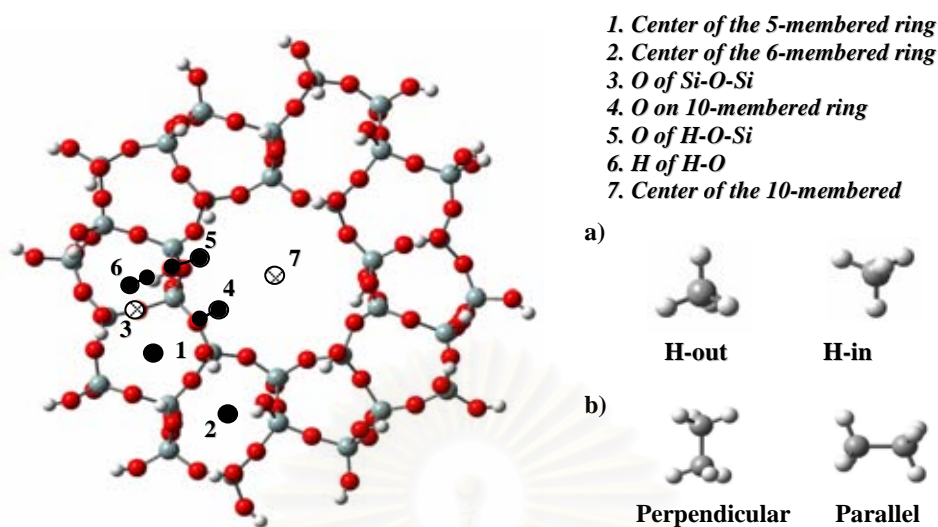
Figure 3.3 The guest molecule was located above and perpendicular to the points labeled by 1-7: a) methane molecule in two configurations, H-in and H-out b) ethane molecule in two configurations, perpendicular and parallel.

The binding energy is defined according to the supermolecular approach as shown in equation 3.2:

$$\Delta E_{bind} = E_{cpx} - E_g - E_s \tag{3.2}$$

where, E_{cpx} is the total energy of the complex while E_g and E_s are the total energy of the guest molecule and of the fragment-surface, respectively. The calculations were performed using GAUSSIAN03 program[56].

The selected data points yielded from the ONIOM(MP2:HF) calculations using the extended 6-31G(d) basis sets were fitted to the analytical function of the form:

$$\Delta E(\text{g,s}) = \sum_i \sum_j \left\{ -\frac{A_{ij}}{r_{ij}^6} + \frac{B_{ij}}{r_{ij}^{12}} + \frac{C_{ij}}{r_{ij}^3} + \frac{q_i q_j}{r_{ij}} \right\} \tag{3.3}$$

where g and s denote guest molecule and the silicalite-1 surface, respectively. The constants A_{ij}, B_{ij} and C_{ij} are fitting constant and r_{ij} is the distance between atom i of guest molecule and atom j of silicalite-1. Here, q_i and q_j are the atomic net charge of

atoms *i* and *j* in atomic units, as obtained from the population analysis of the isolated molecules in the quantum chemical calculations.

3.2 Molecular Dynamics Simulations

The crystallographic cell of silicalite-1[57] contains Si and O atoms, with lattice parameters $a = 20.07$ Å, $b = 19.92$ Å, and $c = 13.42$ Å. Periodical boundary conditions are applied to avoid finite size effects. Simulations have been carried out for the consisting system of 4 silicalite-1 unit cells (1 x 2 x 2 unit) to represent the straight channel. The statistical mechanics ensemble employed is the microcanonical (NVE) ensemble. The trajectories have been calculated by the use of the velocity version of the Verlet algorithm. Numbers are set to 8, 16 and 32 molecules per unit cell, corresponding to 32, 64 and 128 molecules per simulation box. It has been found that the flexibility of the lattice does not significantly increase small guest diffusion. Thus, the silicalite lattice was allowed to remain rigid through out the simulation. The time step was 0.5 fs and the evaluation part of each run corresponds to a length of 2.5 ns after a 5 ps thermalization period. The average temperature of the system was 300 K.

The methane-silicalite interactions are described by our quantum *ab initio* fitted potential models. Methane-methane and methane-channel potentials have been taken from Fritzsche *et al.*[58].

CHAPTER IV

RESULTS AND DISCUSSIONS

4.1 *Ab Initio* Fitted Potential Functions

The quantum *ab initio*, ONIOM(MP2/6-31G(d):HF/6-31G(d)) method as well as the BSSE correction, have been applied to investigate the interaction between guest molecules and the (010) external surface of silicalite-1. As given in details in the calculation methods (chapter III), the selected data points of the energies calculated for various positions and orientations of guest molecule on the surface were generated. The calculated value for the pair interaction energy, ΔE, were fitted, multidimensional non-linear least-squares procedure, to function consisting of a Lennard-Jones, a Coulombic and additional polynomial term.

4.1.1 Guest/Silicalite-1

4.1.1.1 The Optimal Function and Set of Parameters

About 200 selected data points obtained from ONIOM calculations with BSSE corrections were fitted to the analytical function of the form:

$$\Delta E(\text{m,s}) = \sum_i \sum_j \left\{ -\frac{A_{ij}}{r_{ij}^6} + \frac{B_{ij}}{r_{ij}^{12}} + \frac{C_{ij}}{r_{ij}^3} + \frac{q_i q_j}{r_{ij}} \right\} \tag{4.1}$$

$$\Delta E(\text{e,s}) = \sum_i \sum_j \left\{ -\frac{A_{ij}}{r_{ij}^6} + \frac{B_{ij}}{r_{ij}^{12}} + \frac{C_{ij}}{r_{ij}^5} + \frac{q_i q_j}{r_{ij}} \right\} \tag{4.2}$$

where m, e and s denote methane molecule, ethane molecule and the silicalite-1 surface, respectively. The constants A_{ij}, B_{ij} and C_{ij} are fitting constant and r_{ij} is the distance between atom i of methane and atom j of silicalite-1. Here, q_i and q_j are the atomic net charge of atoms i and j in atomic units, as obtained from the population

analysis of the isolated molecules in the quantum chemical calculations. Besides $-A/r^6$ and B/r^{12} terms, the third polynomial term C/r^3 and C/r^5 were essentially introduced in order to obtain better numerical fitting for the methane and ethane systems, respectively. The final parameter values were summarized in Tables 4.1 and 4.2.

Table 4.1 Fitting parameters for atom i of methane interacting with atom j of the (010) silicalite-1 surface.

i	j	q_i	q_j	A (Å^6kJ/mol^{-1})	B (Å^{12}kJ/mol^{-1})	C (Å^3kJ/mol^{-1})
C	Si	-0.66	1.49	-32.706460	54221801.48075	-1169.27445
C	O	-0.66	-0.80	8355.16690	2587679.88528	668.43642
C	H	-0.66	0.48	-1678.48834	5034.78319	-228.18617
H	Si	0.16	1.49	1952.80808	41123.63272	233.86862
H	O	0.16	-0.80	-1262.12699	31830.76176	-136.54700
H	H	0.16	0.48	-2.03914	666.51147	40.35601

Table 4.2 Fitting parameters for atom i of ethane interacting with atom j of the (010) silicalite-1 surface.

i	j	q_i	q_j	A (Å^6kJ/mol^{-1})	B (Å^{12}kJ/mol^{-1})	C (Å^5kJ/mol^{-1})
C	Si	-0.47	1.49	-1003.97913	24466910.30377	-16221.55618
C	O	-0.47	-0.80	-6528.25350	895969.74430	1068.04826
C	H	-0.47	0.48	2546.63288	163490.53037	214.82663
H	Si	0.16	1.49	23653.62039	2799222.56861	10214.80332
H	O	0.16	-0.80	-4880.70655	20124.82982	-2242.81814
H	H	0.16	0.48	673.63628	3934.73603	365.32587

Although, the fitting parameters for $-A/r^6$ was not able to forced to be negative in order to represent attractive interactions of the pair, but the repulsive term B/r^{12} was controlled to be positive in order to avoid unwanted negative hole at short distances due to a much higher slope of the B/r^{12} term than that the $-A/r^6$, C/r^3 and C/r^5.

4.1.1.2 Quality of the Fitted Functions

The physical meaning as well as quality of the guest/silicalite-1 function is considered from its ability in representing *ab initio* data. An advantage of this approach is that it is a one-to-one correspondence between the predicted (by the potential function) and the observed (by the *ab initio* calculations) interaction energies.

In Figures 4.1 - 4.4, potential energy curves for various methane and ethane orientations were shown, respectively. As can be seen from Figure 4.1, the methane/silicalite-1 fitted potentials (ΔE_{Fitted}). In the H-in configuration where one H atom of methane points perpendicular to the surface (see Figure 3.3 for details), the lowest binding energy (-4.33 kJ/mol) takes place when CH_4 moved along trajectory 7. The shortest distance (4 Å) was found when CH_4 approaches to H atom of the silanol group trajectory 5 which the lowest energy to the surface atom of -0.32 kJ/mol. Similar conclusion can be also made for the methane/silicalite-1 binding when CH_4 is in H-out configuration, one hydrogen point out and perpendicular to the silicalite-1 surface (Figure 4.2). Slightly differences were found in terms of binding energy and distance in which the energy minima are slightly lower and the corresponding distances are slightly longer in the H-out then those of the H-in configuration.

The ΔE_{ONIOM} and ΔE_{Fitted} for the ethane/silicalite-1 were shown in Figures 4.3 – 4.4. Beside a good agreement among the two types of interaction energies, discrepancy was somehow taken place for the trajectories 1, 2 and 5 in Figure 4.3 (C_2H_6 lies perpendicular to the silicalite-1 surface, see Figure 3.3) where the ΔE_{Fitted} overestimate the ΔE_{ONIOM} and vice versa for trajectory 4. However, this is the best fit one can do according to equation 4.2 under the condition that the r^{-12} term was forced to give position sign and only one polynomial term (r^{-5}) was included in the standard interatomic function functional (Lennard-Jone plus Coulombic terms). Adding more term can also create unwanted minima due to an increase of degree of freedom in the numerical fitting. However, the above mentioned errors would play very minor role

and should not affect the simulation results because such discrepancy is relative small compared to the binding energy of lower than -10 kJ/mol when C_2H_6 move along trajectory 7 into center of the straight channel. In the other word, C_2H_6 would not adsorb on the (010) silanol covered silicalite-1 surface but would be rather mobile via moving above the surface and move smoothly through the center of the straight channel.

The ΔE_{ONIOM} is better represented by the ΔE_{Fitted} (Figure 4.4) when C_2H_6 lies parallel to the surface (see Figure 3.3 for definition). As expected, the energy minima are slightly higher and the corresponding distances are slightly longer for the parallel compare to those of the perpendicular configuration.

The correlation between ΔE_{ONIOM} and ΔE_{Fitted} was plotted in Figures 4.5, in order to illustrate the quality of the fitting for various interaction energy ranges. It can be clearly seen that two sources of energy data for both methane/silicalite-1 and ethane/silicalite-1 are in good agreement especially in the low energy region which plays important role for the molecular dynamics study.

To seek for the unwanted minima and to examine quality of the fitted potentials, the energy contour plot where CH_4 and C_2H_6 molecules are 2 Å, 1 Å and 0 Å above the surface were calculated and plotted (Figure 4.6 – 4.11). Here CH_4 lies in the H-in configuration and C_2H_4 move perpendicular to the surface. The given distance is between C atom of CH_4 center of the C-C bond of C_2H_6 to the nearest H atom of silanol on the surface of silicalite-1. The plots were examine for both situations, with or without silanol groups. In the later case, the guest-surface distance is the same as that of the first case, i.e., the same coordinates of CH_4 or C_2H_6 were used for both calculations. Note that the empirical force field parameters for the surface without silanol were taken from Fritzsche et al.[58].

The contour plots in Figure 4.6-4.11 show low and high energy areas when guest molecules move above the surface at difference distances. Moving along trajectory 7 (Figure 3.3) which is perpendicular to the straight channel, show, as expected, lowest binding energy. This is true for every levels of guest molecules above the surface. When the guest molecules were above the surface 2 Å (Figures 4.6 and 4.9), the surface without silanol gives lower energy and wider negative area than those with silanol. For lower levels (Figures 4.7, 4.8, 4.10 and 4.11), the silanol surface has less effect, i.e., almost the whole surface displays strong repulsion. These agree well with the 2D plots shown in Figures 4.1 – 4.4 where the potential energy

curves show the weak repulsion around the 10-oxygen membered ring and the strong attraction at the center of 10-oxygen membered ring.
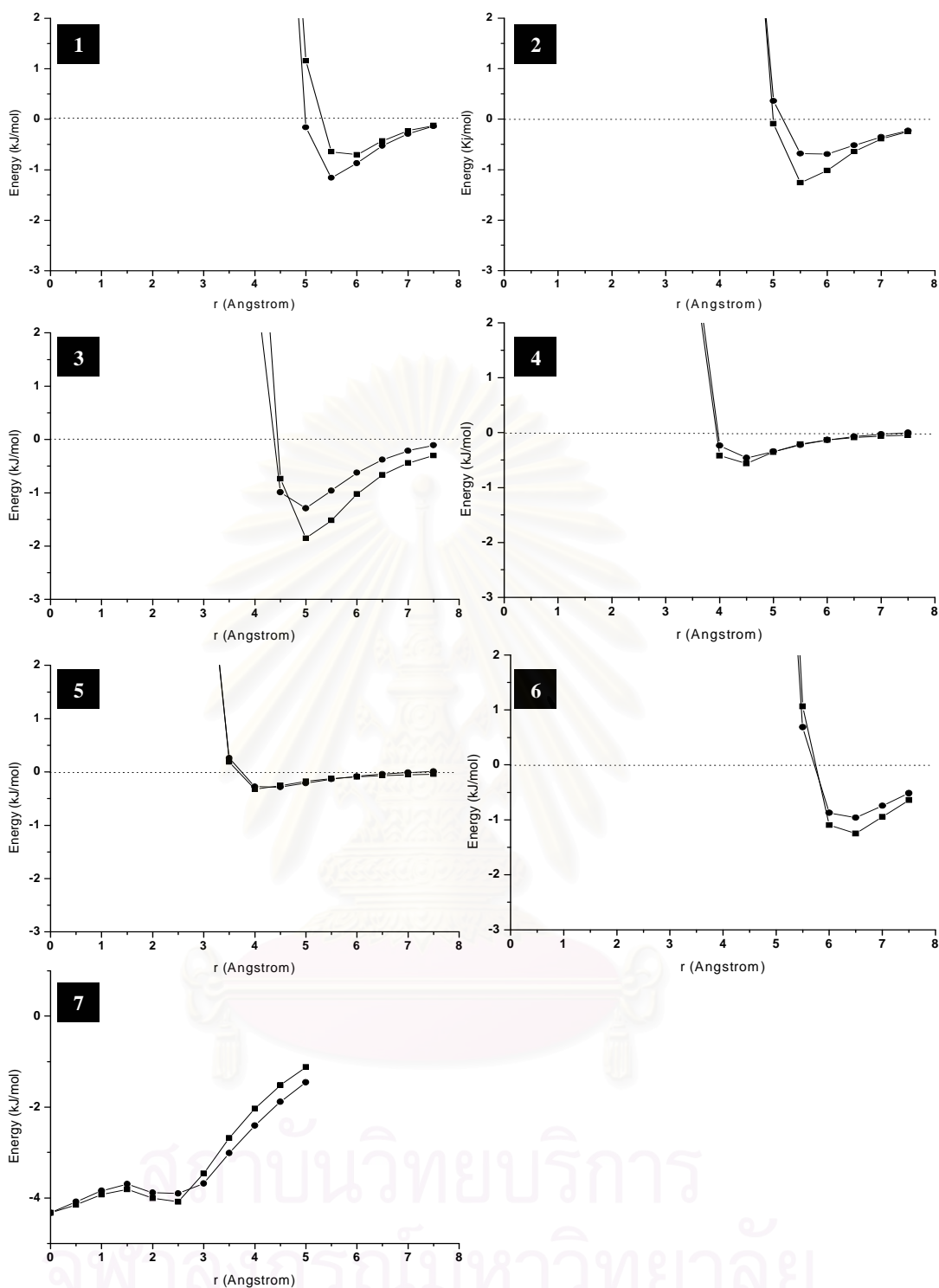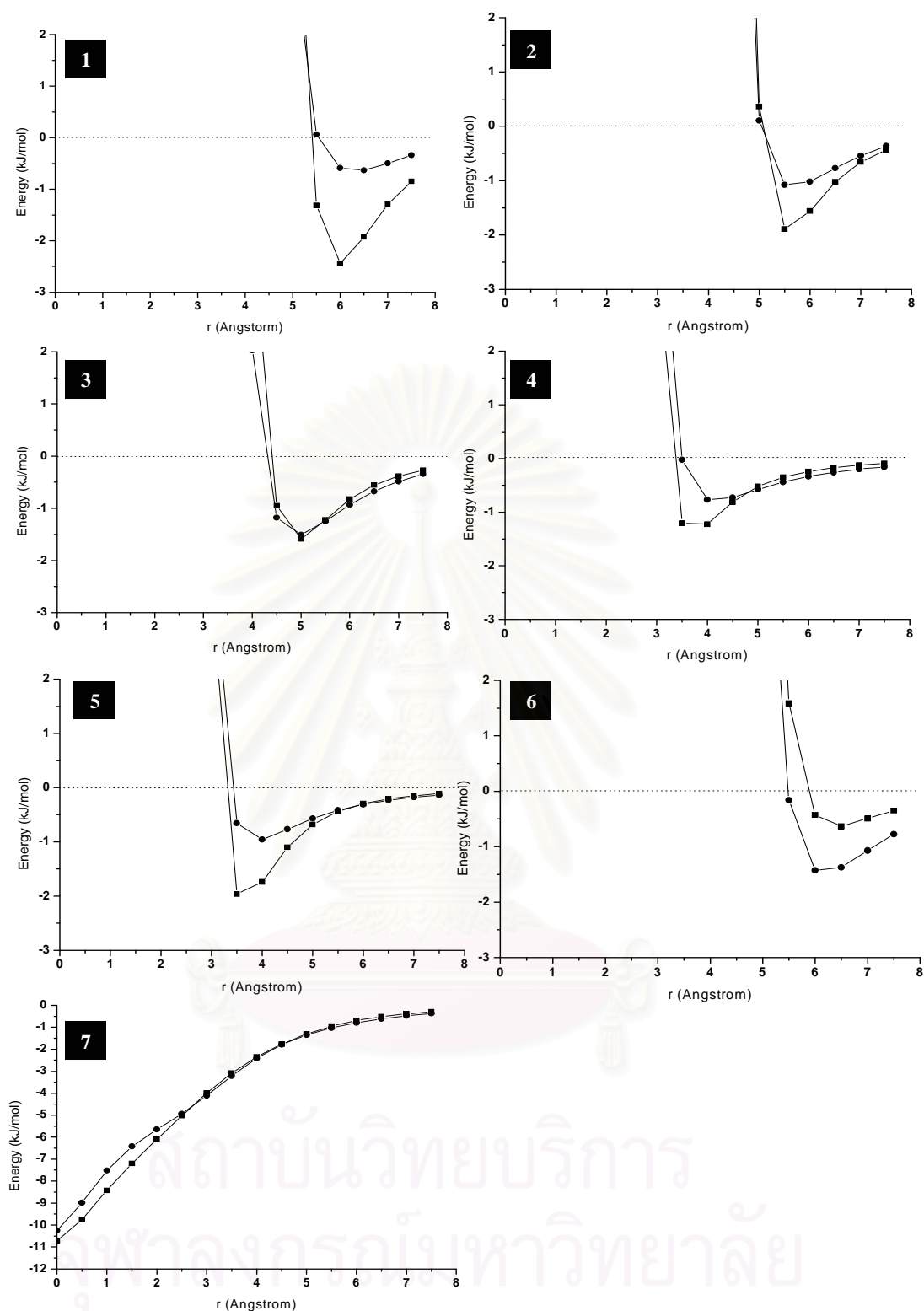
Figure 4.1 Methane/silicalite-1 interaction energies obtained from the ONIOM method (■) and fitted potential calculations (●) using equation 4.1 with the fitted parameters summarized in Table 4.1 in which labels 1 – 7 denote methane trajectory 1 – 7 defined in Figure 3.3 where methane is in H-in configuration. The interatomic distances were between C atom of methane and 1- 7 atoms or center of the ring defined in Figure 3.3.
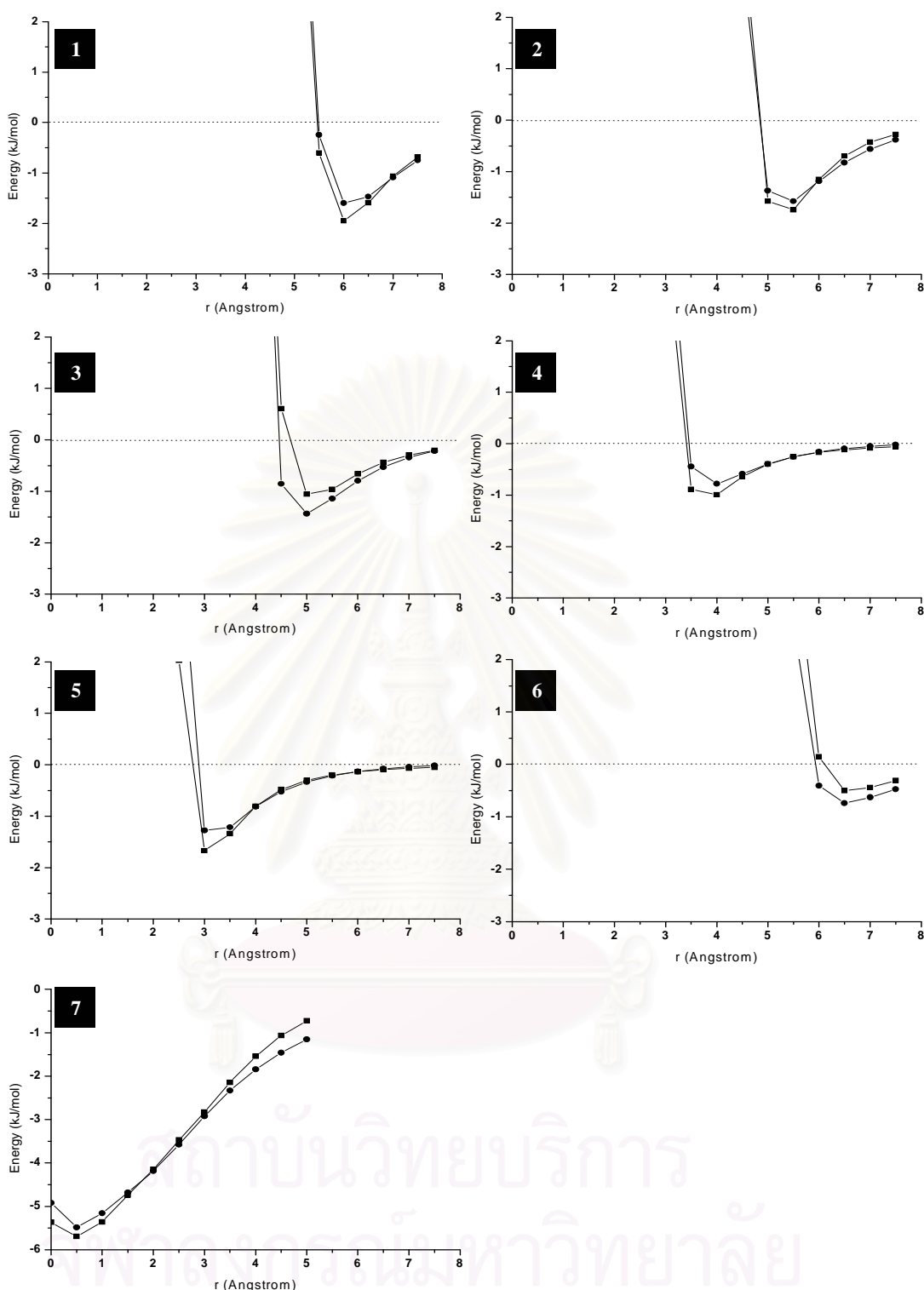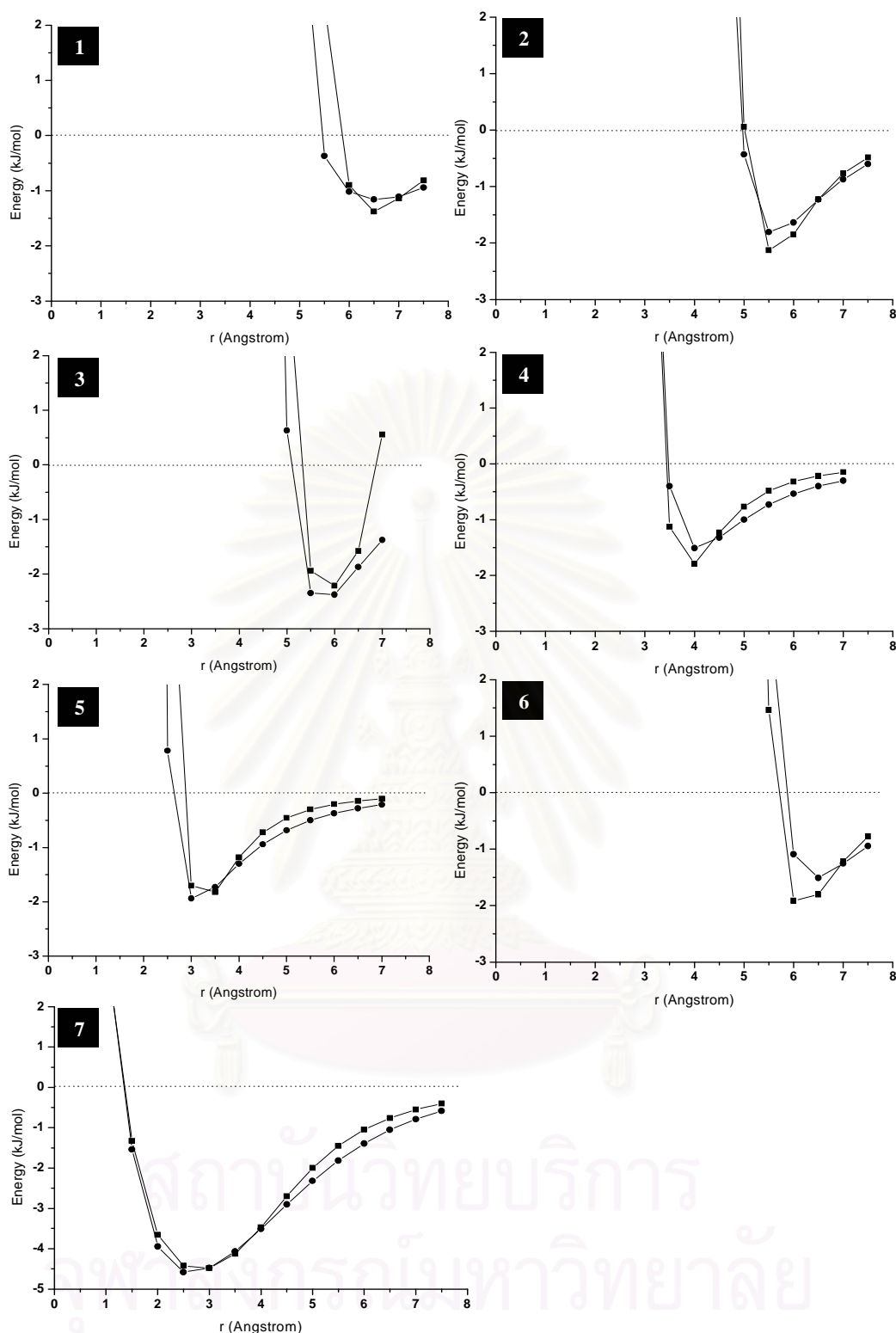
Figure 4.2 Methane/silicalite-1 interaction energies obtained from the ONIOM method (■) and fitted potential calculations (●) using equation 4.1 with the fitted parameters summarized in Table 4.1 in which labels 1 – 7 denote methane trajectory 1 – 7 defined in Figure 3.3 where methane is in H-out configuration. The interatomic distances were between C atom of methane and 1- 7 atoms or center of the ring defined in Figure 3.3.

Figure 4.3 Ethane/silicalite-1 interaction energies obtained from the ONIOM method (■) and fitted potential calculations (●) using equation 4.1 with the fitted parameters summarized in Table 4.1 in which labels 1 – 7 denote methane trajectory 1 – 7 defined in Figure 3.3 where methane is in perpendicular configuration. The interatomic distances were between center of the C-C atom of ethane and 1- 7 atoms or center of the ring defined in Figure 3.3.

Figure 4.4 Ethane/silicalite-1 interaction energies obtained from the ONIOM method (■) and fitted potential calculations (●) using equation 4.1 with the fitted parameters summarized in Table 4.1 in which labels 1 – 7 denote methane trajectory 1 – 7 defined in Figure 3.3 where methane is in pearallel configuration. The interatomic distances were between center of the C-C atom of ethane and 1- 7 atoms or center of the ring defined in Figure 3.3.
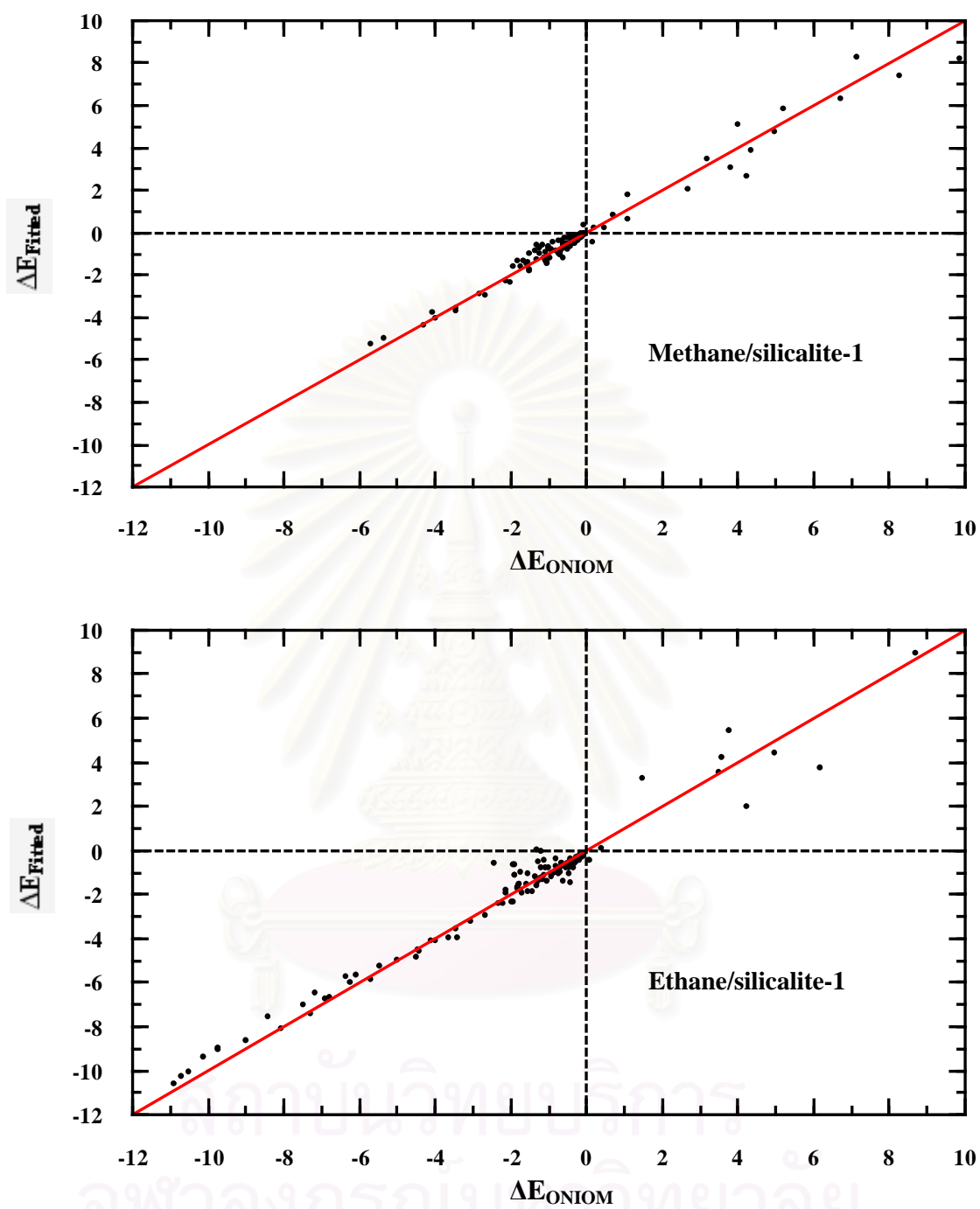
Figure 4.5 Energy data obtained from the ONIOM calculation versus those from fitted potentials for the methane/silicalite-1 and ethane/silicalite-1 systems.
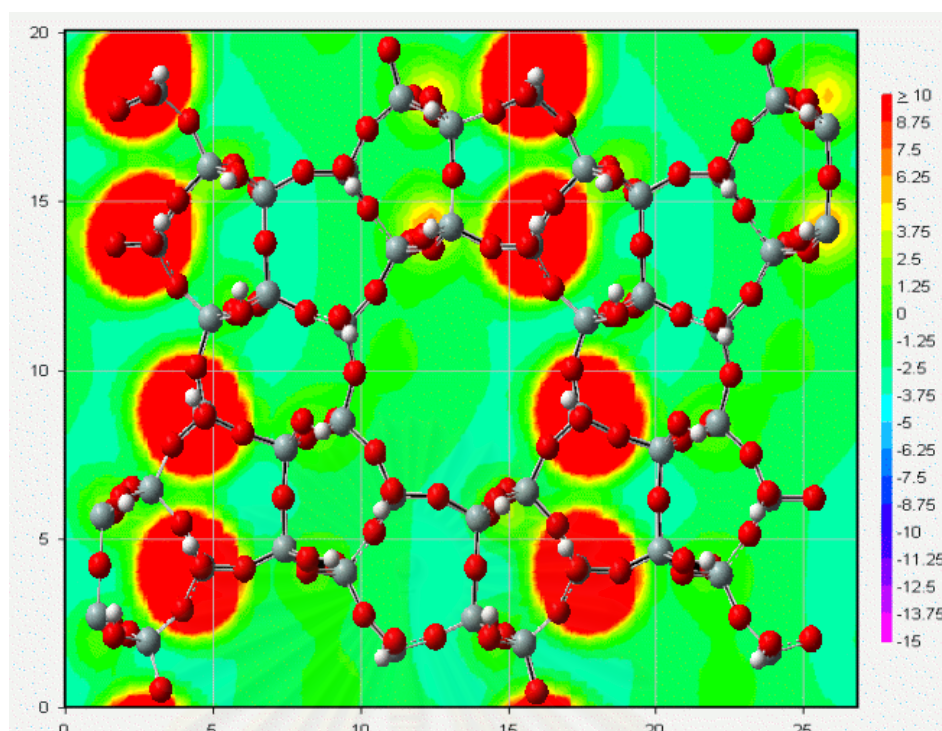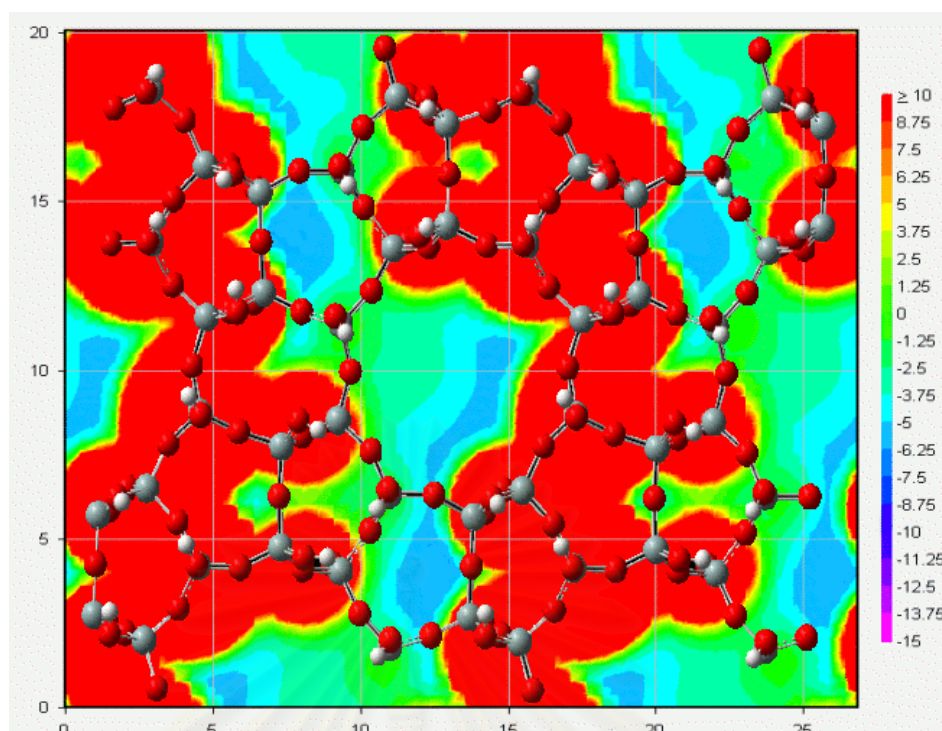
(a) With silanol
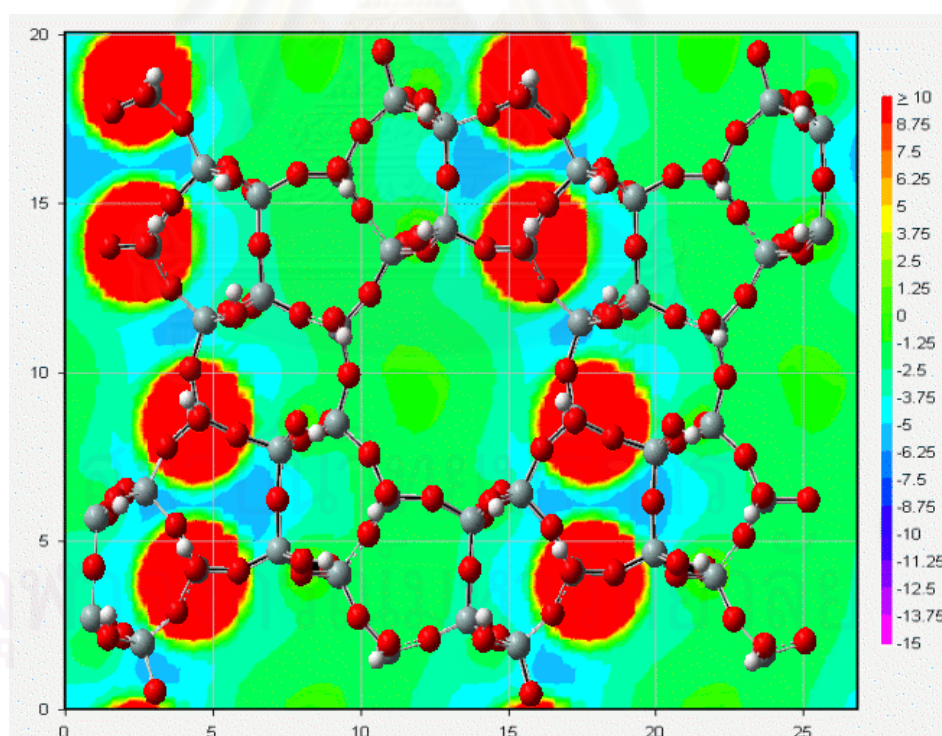
(b) Without silanol

Figure 4.6 Energy contour plots when methane molecule moves above the surface 2 Å for with (a) and without (b) silanol.

(a) With silanol

(b) Without silanol

Figure 4.7 Energy contour plots when methane molecule moves above the surface 1 Å for with (a) and without (b) silanol.

(a) With silanol

(b) Without silanol

Figure 4.8 Energy contour plots when methane molecule moves in the surface plane for with (a) and without (b) silanol.
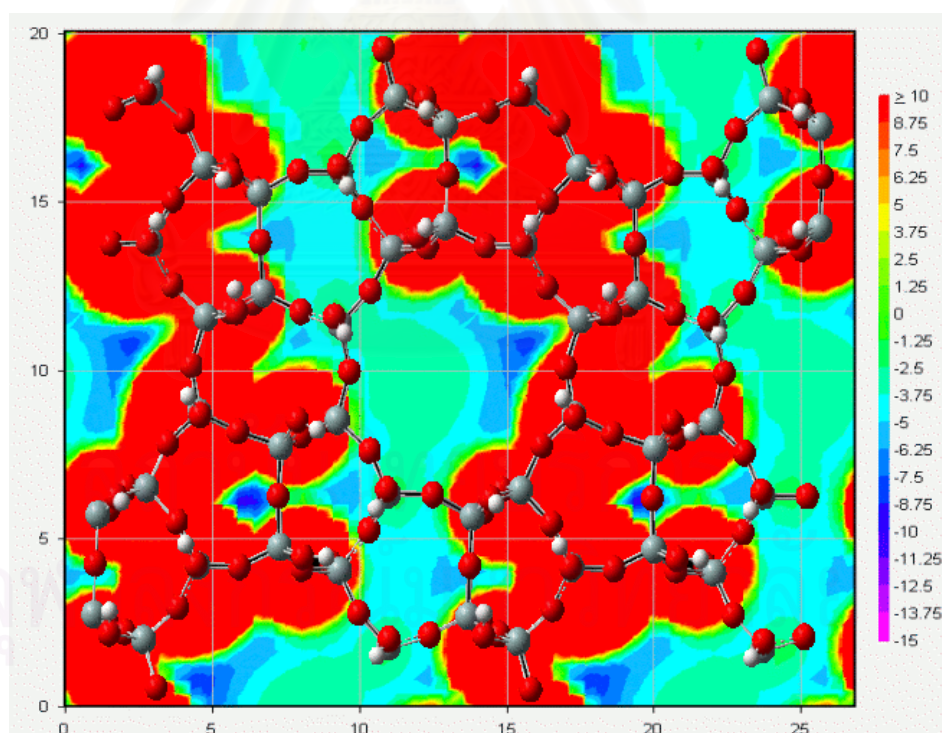
(a) With silanol

(b) Without silanol

Figure 4.9 Energy contour plots when ethane molecule moves above the surface 2 Å for with (a) and without (b) silanol.

(a) With silanol

(b) Without silanol

Figure 4.10 Energy contour plots when ethane molecule moves above the surface 1 Å for with (a) and without (b) silanol.

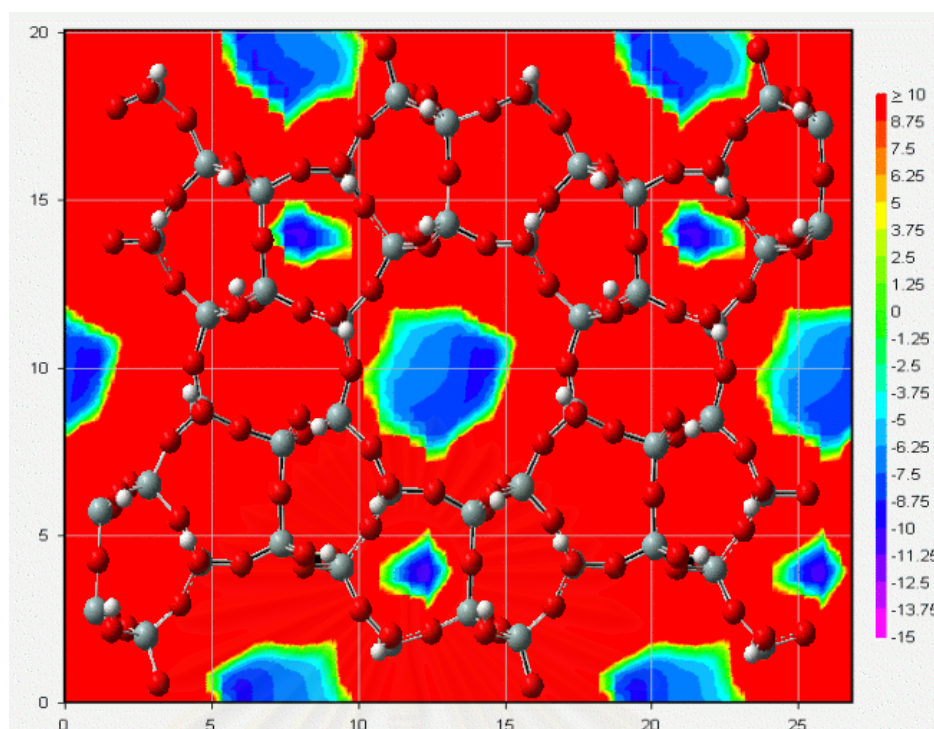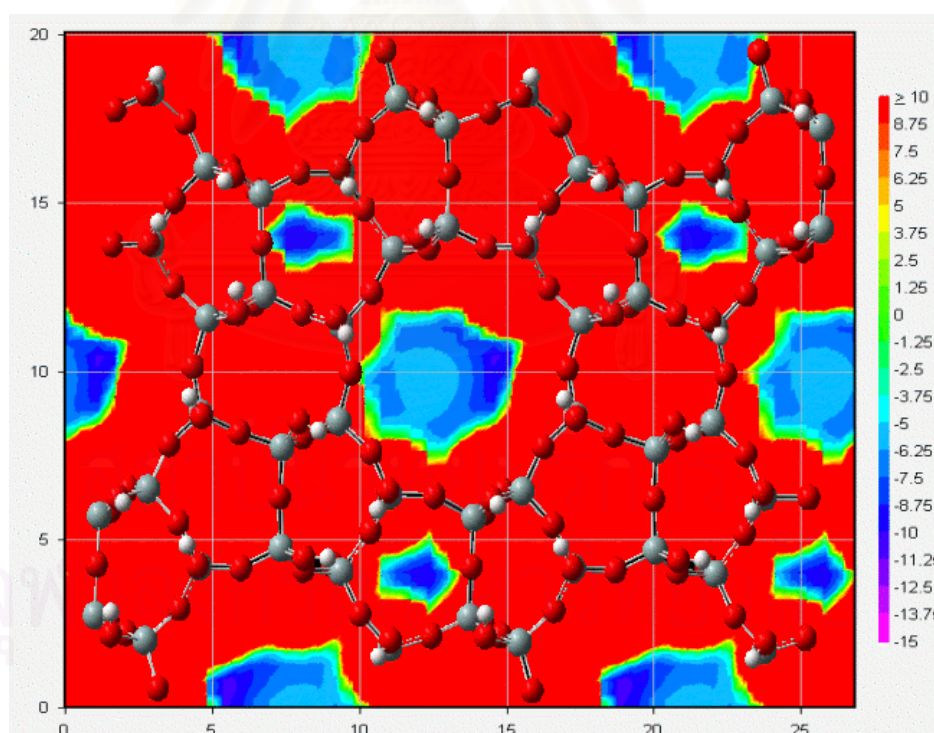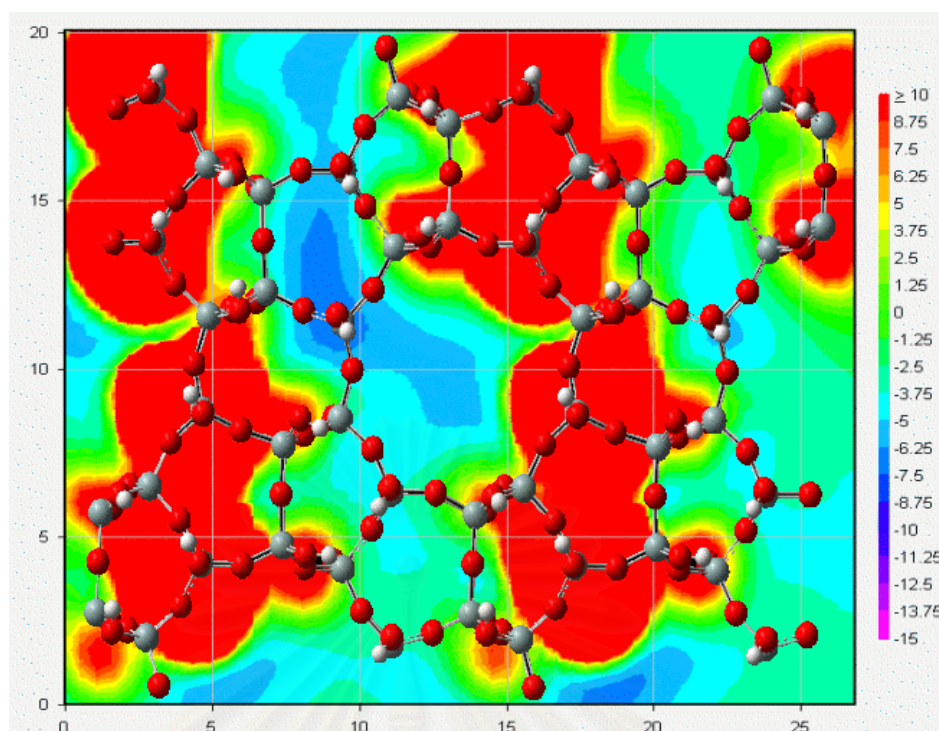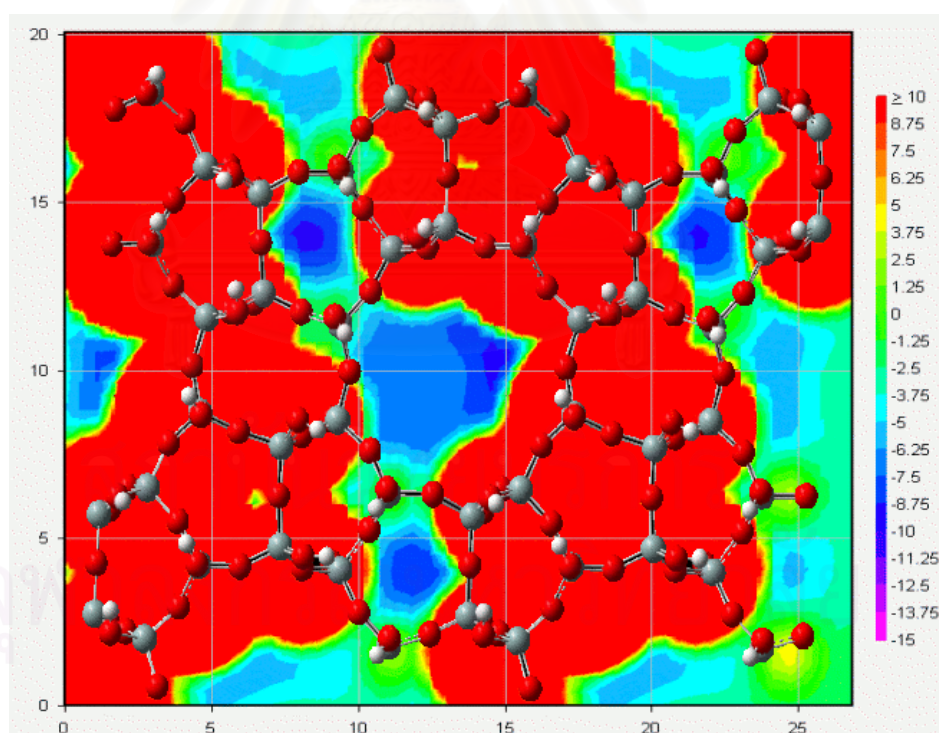**(a) With silanol**

(b) Without silanol

Figure 4.11 Energy contour plots when ethane molecule moves in the surface plane for with (a) and without (b) silanol.
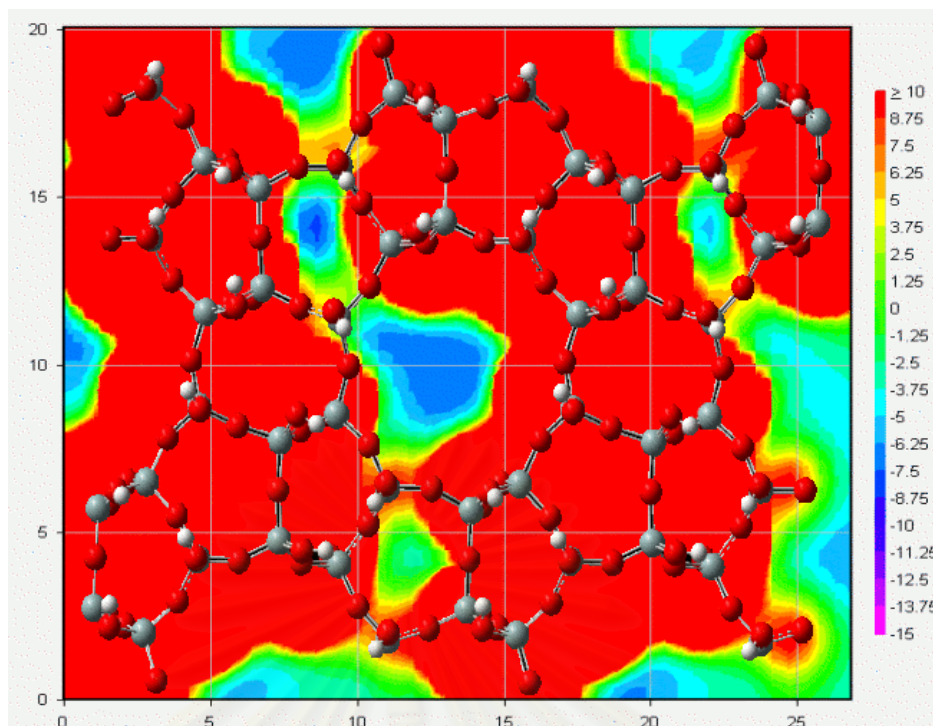
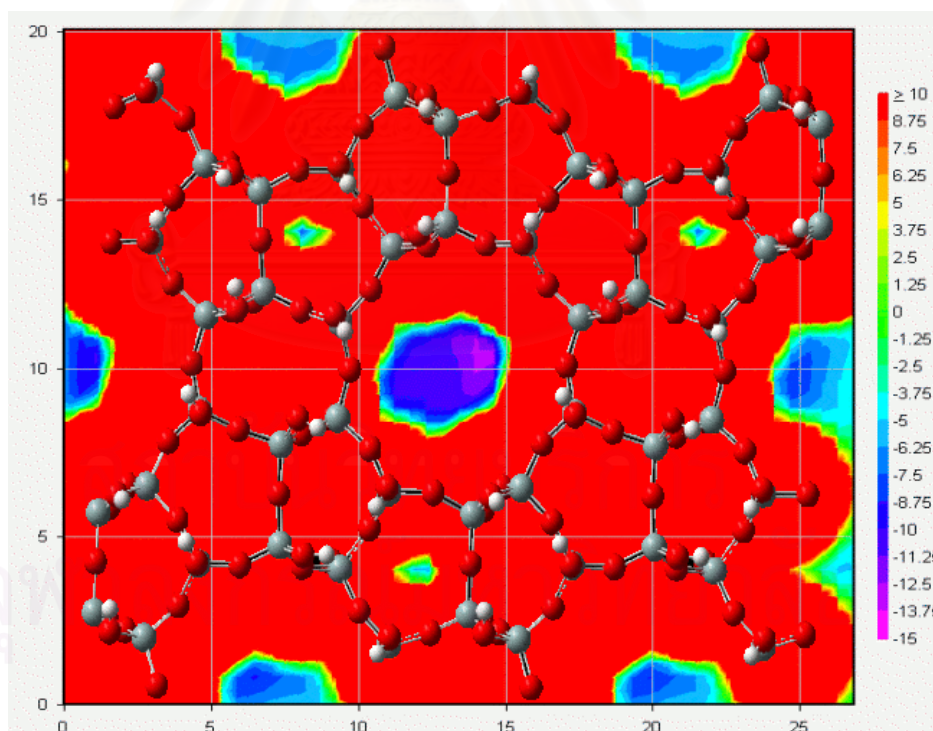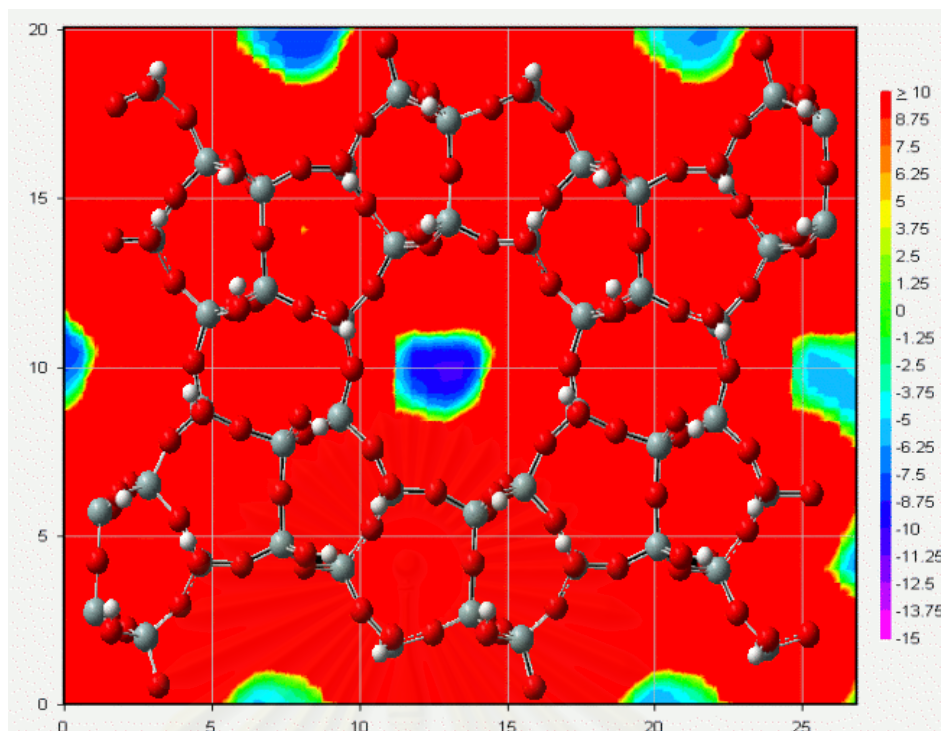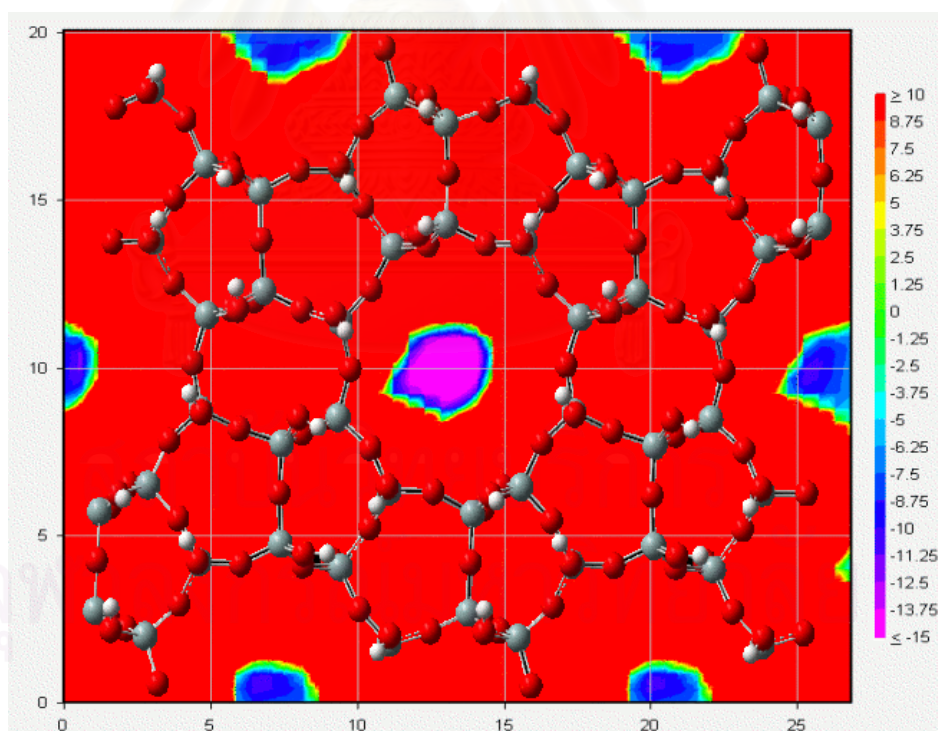**4.2 Validation of the Fitted Potential**

The MD simulations using the newly developed potential functions require the use of in-house software. That is out of the scope of this M.Sc. thesis. However, reliability of this function can not be able to validated without performing the simulations. Therefore, the preliminary MD results given here were taken from part of Thompho Ph.D. thesis where our fitted function was applied. Detailed simulations as well as preliminary results were given in Appendix A.

4.3 Methane/silicalite-1 and Ethane/silicalite-1 Interaction Energies when Entering into Silicalite-1 Channel

As shown in Figures 4.1 – 4.4 and discussed previously, the optimal route for methane and ethane molecules is to approach to the center of 10-oxygen membered ring (trajectory 7 in Figure 3.3). To understand detailed behavior of guest molecules via moving through this channel, binding energies for the methane/silicalite-1 and ethane/silicalite-1 complexes were examined. Calculations were carried out for the two configurations of C_2H_6 molecule, perpendicular and parallel to the surface, using the same method as that used for the development of the potential functions, ONIOM(MP2/6-31G(d):HF/6-31G(d)) with BSSE corrections. For the CH_4 system, the results were taken from ref 16.

Considering Figure 4.12 that taken from Remsungnen *et al.*[59], the methane moves to the center of the straight channel, in the two configurations. In the configuration H-in (solid line in Figure 4.12), the first minimum was detected at the distance (from center of methane to center of 10-oxygen membered ring) of 2.90 Å. At short distance, repulsion between the H atoms of methane ring leads to a slight increase of the binding energy. After a broad maximum at the distance of 1.80 Å, the binding energy, again, decreases and remains constant at -4.14 kJ/mol between the distance of 0.0 -1.50 Å (minus value of the distance denotes the position where the methane molecule is under the surface). Note that at the distance of 0.0 Å in the H-in configuration, the methane is located at the center of the straight channel. For the H-out configuration, the binding energy decreases rapidly when the distance decreases. The minimum was found when the three hydrogen atoms of methane are in the 10-oxygen membered ring plane; i.e., the distance to the center of methane is 0.60 Å and

the corresponding energy is -5.75 kJ/mol. At the distance less than 0.60 Å, the energy, again, increased. The H-out configuration gives a binding energy identical to that of the H-in one, -4.15 kJ/mol, when the methane locates below the surface for -1.00 Å and one of the H-atom lies in the silicalite-1 surface.
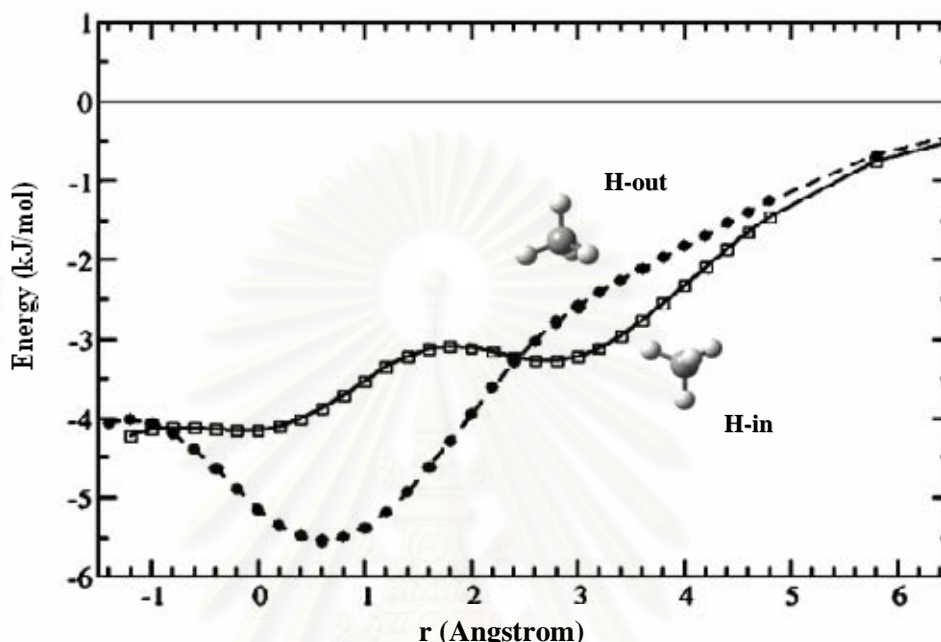
Figure 4.12 Binding energies when the methane molecule is in the configurations H-in and H-out and moves perpendicular to the center of 10-oxygen membered ring (see also Figure 3.3).

Considering our results for C_2H_6, in the perpendicular configuration of ethane (Figure 4.13), the binding energy decreases when the distance decreases. The optimum was found at the center of 10-oxygen membered ring and the corresponding energy is -10.92 kJ/mol. The binding energy, again, increases when the ethane molecule is located between -1.0 and -5.0 Å (minus value means ethane molecule below the surface). In the parallel configuration, the binding energy and distance corresponding to the first minimum are -4.48 kJ/mol and 3.0 Å, respectively. Repulsion between ethane in this configuration and the 10-oxygen membered ring leads to a rapid increase of the binding energy. The highest binding energy is at -0.5 Å and the corresponding binding energy is 16.42 kJ/mol. The binding energy, again, decreases, when ethane is under the surface between -1.0 Å and -3.0 Å. The parallel

configuration gives the lowest binding energy, -7.52 kJ/mol, when the position of ethane is below the surface -3.0 Å.

Regarding the energy minima at the center of the 10-oxygen membered ring of -5.75 kJ/mol for CH_4 and -10.92 kJ/mol for C_2H_6, a clear conclusion is that C_2H_6 can easier enter into the pore mouth of the straight channel of silicalite-1 via the (010) silanol covered surface. The optimal configuration for CH_4 molecule is to point one H atom perpendicular to the silicalite-1 surface while that of the C_2H_6 is to point the molecule axis perpendicular to the surface.
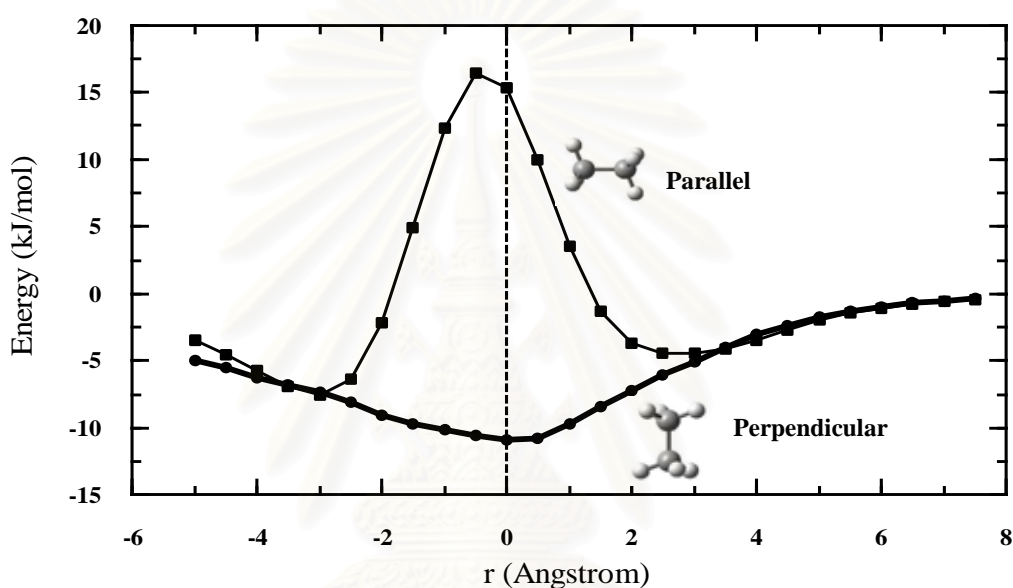
Figure 4.13 Binding energies when the ethane molecule is in the perpendicular and parallel configurations and moves perpendicular to the center of the 10-membered ring (see also Figure 3.3).

CHAPTER V

CONCLUSIONS

Silicalite -1 is an attractive adsorbent for the separation of relatively non-polar species from aqueous media, such as the separation of mixtures of light hydrocarbons with water or other polar solvents. The zeolite external surface is of importance that can affect its catalytic performance. Applications of zeolites usually begin with the initial adsorption of molecules on the external surface of a zeolite crystal followed by diffusion on the external surface and sieving of the molecules into the internal surface. It is known that silanol groups are the key elements determining the adsorption and diffusion behavior of guest molecules on the external surface. Aim of this study is to investigate the interaction between guest molecules and silanol covered silicalite-1 (010) surface in which the *ab initio* fitted potential for the methane/silicalite-1 and ethane/silicalite-1 systems were developed. The (010) external surface of silicalite-1 which is perpendicular to the straight channel was selected. Energy data set for various configurations of guest molecules on the surface were calculated using ONIOM(MP2/6-31G(d):HF/6-31G(d)) method including the correction due to the basis set superposition error (BSSE).

Each energy data set was fitted to the analytical functions. The energies data obtained from ONIOM calculations are in good agreement with those computed from the potential functions. The results from ONIOM calculations show also that the optimal route for methane and ethane molecules is to enter to the straight channel at the center of the 10-oxygen membered ring. The corresponding energies is -5.75 kJ/mol for CH_4 and -10.92 kJ/mol for C_2H_6. The optimal configuration for CH_4 molecule is to point one H atom perpendicular to the silicalite-1 surface while that of the C_2H_6 is to point the molecule axis perpendicular to the surface.

The fitted potential function was examined by Thompho (Ph.D. thesis) using molecular dynamics (MD) simulations in order to validate the fitted functions. The preliminary MD results show the reliability of the function.

REFERENCES

[1] McBain, J. W., *The Sorption of Gases and Vapors by Solids, ch.5*. London: Rutledge, 1932.

[2] Nicholas, J. B., et al., Molecular dynamics simulation of propane and methane in silicalite. *J. phys. Chem.*, 97 (1993): 4149-4163.

[3] Jost, S.; Fritzsche, S. and Haberlabdt, R., An MD study on the diffusion of a mixture of methane and xenon in silicalite. *Chem. Phys. Lett.*, 279 (1997): 385-388

[4] Demontis, P.; Fois, E. S. and Suffritti, G. B., Molecular dynamics studies on zeolites. 4. Diffusion of methane in silicalite. *J. phys. Chem.*, 94 (1990): 4329-4334.

[5] Bussai, C., et al., On the diffusion of water in silicalite-1: MD simulations using ab initio fitted potential and PFG NMR measurements. *Appl. Catal. A.*, 232 (2002): 59-66.

[6] Bussai, C.; Hannongbua, S. and Fritzsche, S., Ab initio potential energy surface and molecular dynamics simulations for the determination of the diffusion coefficient of water in silicalite-1. *Chem. Phys. Lett.*, 354 (2002): 310-315.

[7] Cronstedt, A. F., Akad. Handl. 18 (1756): 120-123.

[8] Kärger, J. and Ruthven, D. M., *Diffusion in Zeolites and Other Microporous Solids*. pp. 604. New York: Wiley, 1992.

[9] Galarneau, A.; Renzo, F. D. and Vendrine, A., *Zeolite and Mesoporous Materials at the Dawn of the 21 st Century, 13th International Conference Montpellier, France*. pp. Amsterdam: Elsevier Science, 2001.

[10] Breck, D. W., *Zeolite Molecular Sieves: Structure, Chemistry, and, Use*. pp. New York: Wiley, 1974.

[11] Hagens, J., *Industrial Catalysis*. pp. 225-244. Wiley-VCH, 1999.

[12] Bonhomme, F.; Welk, M. E. and Nenoff, T. M., Co_2 Selectivity and Lifetimes of High Silica ZSM-5 Membranes. *Microporous and Mesoporous Materials*, 66 (2003): 181-188.

[13] Hedlund, J. Thin Films of Molecular Sieves. Luleå University of Technology, 1998.

[14] Ribeiro, F. R., et al., Structure-Activity Relationship in Zeolites. *J. Mol. Cat.*, 96 (1995): 245-270.

[15] W.M. Meier, M. S., *Molecular Sieves, Society for Chemical Industry*. pp. 10. London: 1968.

[16] Meier, W. M. and Olson, D. H., *Atlas of Zeolites Structure Types*. (3rd), pp. Butterworths, 1992.

[17] Tsai, T.; Liu, S. and Wang, I., Disproportionation and Transalkylation of Alkylbenzenes Over Zeolite Catalysts. *Appl. Catal. A: General*, 181 (1999): 355-398.

[18] McCusker, L. B., et al., The Triple Helix Inside the Large-pore Aluminophosphate Molecular Seive VPI-5. *Zeolites*. 11 (1991): 308-313.

[19] Davis, M. E., et al., A Molecular Sieve with Eighteen-membered Rings. *Nature*. 331 (1988): 698-699.

[20] Davis, M. E., et al., VPI-5: The first molecular sieve with pores larger than 10 Angstroms. *Zeolites*. 8 (1988): 362-366.

[21] Baerlocher, C.; Meier, W. M. and Olson, D. H., *Atlas of Zeolite Framework Types*. pp. 1. Elsevier, Amsterdam, 2001.

[22] Satterfield, C. N., *Heterogeneous Catalysis in Industrial Practice*. pp. 107-108, 226-240, 420-421. Krieger publishing company, 1996.

[23] Turro, N. J., et al., Photochemical and Magnetic Resonance Investigations of the Supramolecular Structure and Dynamics of Molecules and Reactive Radicals on the External and Internal Surface of MFI Zeolites. *J. Am. Chem. Soc*, 122 (2000): 11649-11659.

[24] Armaroli, T., et al., FTIR study of the interaction of some branched aliphatic molecules with the external and internal sites of H-ZSM5. *Phys. Chem. Chem. Phys.*, 3341-3348 (2000).

[25] Armaroli, T., et al., A study of the external and internal sites of MFI-type zeolitic materials through the FT-IR investigation of the adsorption of nitriles. *Appl. Catal. A.*, 216 (2001): 59-71.

[26] Suzuki, I.; Namba, S. and Yashima, T., Determination of External surface Area of ZSM-5 Type Zeolite. *J. Catal.*, 81 (1983): 485-492.

[27] Csicsery, S. M., Types of Shape Selectivities. *Appl. Chem.*, 58 (1986): 841.

[28] Liu, Z., et al., Characterization of the External Surface of Silicalites Employing Paramagnatic Resonance. *J. Phys. Chem. A*, 108 (2004): 8040-8047.

[29] Campbell, S. M.; Jiang, X. Z. and Howe, R. F., Methanol to Hydrocarbons: Spectroscopic Studies and the Significant of Extra-framwork Aluminium. *Mic. Mes. Mat.*, 29 (1999): 91-108.

[30] Makwell, I. E. and Stork, W. H. J., *Studies in surface science and catalysis, in: Introduction to Zeolite Science and Practice.* (2nd ed.), pp. 747. 2001.

[31] Govind, N., et al., Zeolite-Catalyed Hydrocarbon Formation from Methanol: Density Functional Simulation. *Int. J. Mol Sci.*, 3 (2002): 424-434.

[32] Mellot, C. F. and Cheetam, A. K., Energetics and structure of fluoro- and chlorofluorocarbons in zeolites: Forcefield development and Monte Carlo simulations. *J. Phys. Chem. B*, 103 (1999): 3864.

[33] Macedonia, M. D., et al., Adsorption Studies of Methane, Ethane, and Argon in the Zeolite Mordenite: Molecular Simulations and Experiments. *Langmuir*, 16 (2000): 3823-3834.

[34] Demontis, P., et al., Molecular dynamics studies on zeolites. 6. Temperature dependence of diffusion of methane in silicalite. *J. phys. Chem.*, 96 (1992): 1482-1490.

[35] Demontis, P.; Suffritti, G. B. and Mura, P., A molecular dynamics study of diffusion of methane in silicalite molecular sieve at high dilution. *Chem. Phys. Lett.*, 191 (1992): 553-560.

[36] Goodbody, S. J., et al., Molecular Simulation of Methane and Butane in Silicalite. *J. Chem. Soc. Faraday Trans.*, 87 (1991): 1951-1958.

[37] June, R. L.; Bell, A. T. and Theodorou, D. N., A Molecular Dynamics Study of Methane and Xenon in Silicalite. *J. Phys. Chem.*, 94 (1990): 8232-8240.

[38] Catlow, C. R. A., et al., Molecular Dynamics Studies of Hydrocarbon Diffusion in Zeolites. *J. Chem. Soc. Faraday Trans.*, 87 (1991): 1947-1950.

[39] Dumont, D. and Bougeard, D., A molecular dynamics study of hydrocarbons adsorbed in silicalite. *Zeolites*, 15 (1995): 650-655.

[40] Yashonath, S.; Demontis, P. and Klein, M. L., A molecular dynamics study of methane in zeolite NaY. *Chem. Phys. Lett.*, 153 (1988): 551-556.

[41] Lara, E. C. d.; Kahn, R. and Goulay, A. M., Molecular dynamics by numerical simulation in zeolites: Methane in NaA. *J. Chem. Phys.*, 90 (1989): 7482-7491.

[42] Maginn, E. J.; Bell, A. T. and Theodorou, D. N., Transport diffusivity of methane in silicalite from equilibrium and nonequilibrium simulations. *J. Phys. Chem.*, 97 (1993): 4173-4181.

[43] Nowak, A. K., et al., Mobility of adsorbed species in zeolites: methane, ethane, and propane diffusivities. *J. Phys. Chem.*, 95 (1991): 848-854.

[44] Demontis, P.; Suffritti, G. B. and Tilocca, A., Diffusion and vibrational relaxation of a diatomic molecule in the pore network of a pure silica zeolite: a Molecular Dynamics study. *J. Chem. Phys.*, 105 (1996): 5586-5594.

[45] Caro, J., et al., Microdynamics of methane, ethane and propane in ZSM-5 type zeolites. *J.Chem. Soc. Faraday. Trans.*, 1986 (1985): 2541-2550.

[46] Humbel, S.; Sieber, S. and Morokuma, K., The IMOMO Method: Integration of Different Levels of Molecular Orbital Approximations for Geometry Optimization of Large Systems: Test for N-butane Conformation and SN2 Reaction: RCl+Cl⁻. *J. Chem. Phys.*, 105 (1996): 1959-1967.

[47] Svensson, M., et al., ONIOM: A Multilayered Integrated MO+MM Method for Geometry Optimizations and Single Point Energy Predictions. A Test for Diels-Alder Reactions and Pt(P(t-Bu)3)2 + H2 Oxidative Addition. *J. Phys. Chem.*, 105 (1996): 19357-19363.

[48] Maseras, F., Hybrid Quantum Mechanics/Molecular Mechanics Methods in Transition Metal Chemistry. *Top. Organomet. Chem.*, 4 (1999): 165-191.

[49] Vreven, T. and Morokuma, K., On the Application of the IMOMO (Integrated Molecular Orbital + Molecular Orbital) Method. *J. Comp. Chem.*, 21 (2000): 1419-1432.

[50] Morokuma, K., ONIOM and Its Applications to Material Chemistry and Catalyses. *Bull. Kor. Chem. Soc.*, 24 (2003): 797-801.

[51] Vreven, T., et al., Combining Quantum Mechanics Methods with Molecular Mechanics Methods in ONIOM. *J. Chem. Theo. Comp.*, 2 (2006): 815-826.

[52] Lennard-Jones, J. E., Cohesion. *Proceedings of the Physical Society*, 43 (1931): 461-482.

[53] Hobza, P. and Zahradnik, R. Intermolecular Interactions Between Medium-sized Systems. Nonempirical and Empirical Calculations of Interaction Energies: Successes and Failures. *Chem. Rev.*, 88 (1988): 871-897.

[54] Suaer, J., et al., Theoretical Study of van der Walls Complexes at Surface Sites in Comparison with the Experiment. *Chem. Rev.*, 94 (1994): 2095-2160.

[55] Remsungnen, T., et al., Optimal Binding Site of a MEthane Molecule on the Silanol Covered (010) Surface of Silicalite-1: ONIOM Calculations. J. Phys. Chem., 110 (2006): 11932-11935.

[56] Frisch, M. J., et al. *Gaussian 03*, Revision C.02; Wallingford CT: Gaussian, Inc., 2004.

[57] Meier, W. M. and Olson, D. M., Preface. *Zeolites*, 17 (1996): 1-2.

[58] Fritzsche, S., et al., Is There a Coupling Between Rotational and Translational Motion of Methane in Silicalite-1 and $AlPO_4^{-5}$? *Chem. Phys. Lett.*, 411 (2005): 423-428.

APPENDIX

APPENDIX A

PRELIMINARY MOLECULAR DYNAMICS
SIMULATIONS RESULTS

Molecular Dynamics Simulations

A.1 Methane loading

Here, the methane molecules were loaded into the zeolite straight channel through the external surface at 32, 64, and 128 molecules per simulation and at the temperature of 300 K. The simulations were carried out for both environments, with and without silanol groups (see section 3.2 for simulation details).

The numbers of methanes enter into the pore were plotted with respect to the simulation time (Figure A.1). They were rapidly increased in the first 100 ps and fulfilled in the pore at about 200 ps.
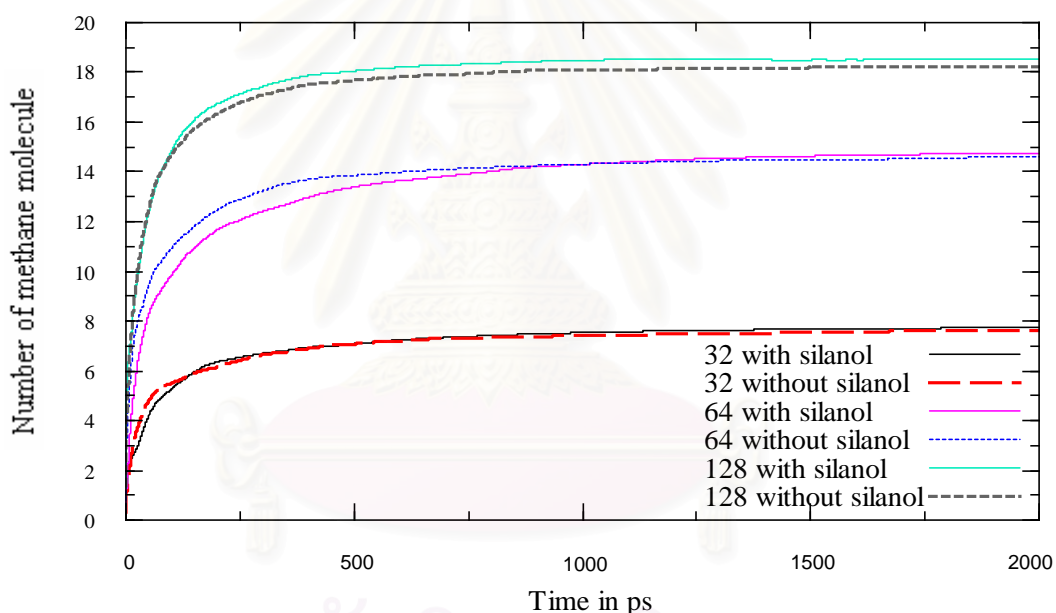
Figure A.1 Numbers of methane molecule entering into the silicalite-1 channel for the simulations with and without silanol (see section 3.2 for calculation detail).

A.2 Sticking Probability

For analyzing the molecular sticking that the guests molecules will be able to enter the intracrystalline space, is a key quantity for the application of such materials in heterogeneous catalysis and molecular sieving. There are two different events of molecular propagation, which are close related to the molecular sticking probabilities:

(1) molecules from gas phase encounters surface (n_1)
(2) molecules from gas phase enters intracrystalline space (n_2)

Denote by n_i the number of events of type i (i = 1, 2), the sticking probability α is defined by

$$\alpha = n_2 / n_1 \qquad\qquad (A.1)$$

The result in Figure A.2 shows the decrease of sticking coefficient as the function of concentration. At low concentration, the system with silanol system gives lower sticking coefficient than that without silanol. That means that the silanol surface is the barrier of the transport of methane molecules into the pore. This effect does not detect at high concentration, this can be due to the fact that the methane molecules inside zeolite pore are packed, while the other methane molecules are assumed to occupy the external surface. Therefore, other methane molecules in the gas phase are rather difficult to move into the intracrystalline phase.
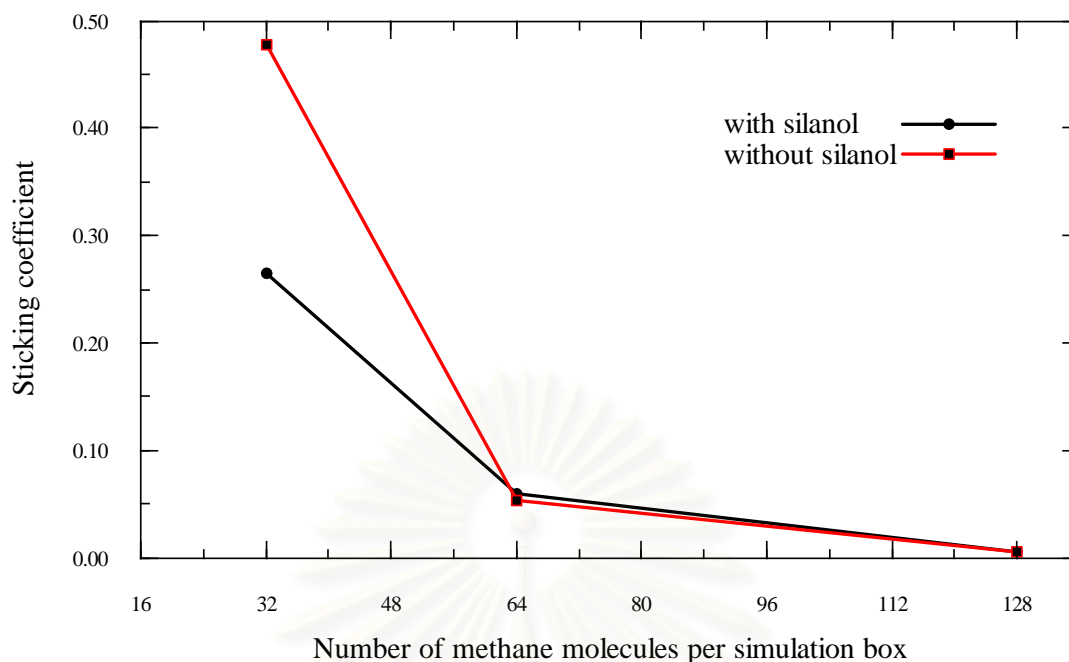
Figure A.2 The sticking coefficients of methane molecules obtain from the simulations with and without silanol group on the silicalite-1 surface.

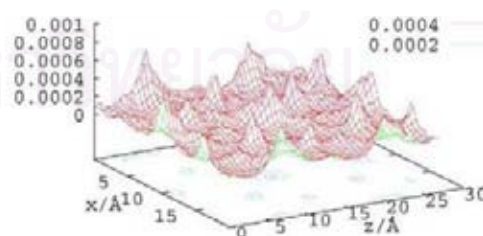**3. Distribution of Methane Molecules on the Silicalite-1 Surface**

Distribution of methane molecules on the (010) external silicalite surface (*xz* plane) are illustrated in Figure A.3. The result presents the density of methane molecules for the systems with (Figure A.3a) and without (Figure A.3b) silanol group. This plot learns us how the influent of silanol group on silicalite surface effects of the diffusion of methane molecules.
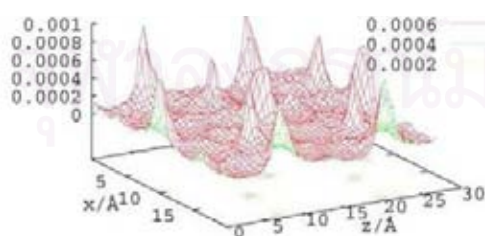
Figure A.3 Density plots of methane molecules on the (010) surface of silicalite-1 for the simulations systems (a) with and (b) without silanol groups.

It can be clearly seen from the plots that this diffusion probability for the system with silanol group system is about two times higher than that without silanol. This mean that methane molecules are rather localized on the silanol covered surface. This is due to stronger binding of methane to the silanol than that to the naked surface. This confirms the diffusion effect shown in Figure A.3 in which the methane molecules on the surface move slower to enter into the silicalite pore.

VITAE

NAME: Rungroj Chanajaree

DATE AND PLACE OF BIRTH: 18 March 1981 in Bangkok, Thailand

ELEMENTARY SCHOOL:

1987-1993   Assumption College Thonburi, Bangkok

SECONDARY SCHOOL:

1993-1996   Assumption College Thonburi, Bangkok

1996-1999   Wat Pradoonaisongtum School, Bangkok

UNIVERSITY EDUCATION:

1999-2002   Diploma in Analytical Chemistry, Institute of Analytical Chemistry Training, Department of Science Service, Ministry of Science, Technology and Environment, Bangkok (Affiliated Institute of Chulalongkorn University)

2002-2004   B. Sc. in Chemistry, Department of Chemistry, Faculty of Science, Chulalongkorn University, Bangkok

2004-2007   M. Sc. in Physical Chemistry, Department of Chemistry, Faculty of Science, Chulalongkorn University, Bangkok